

NON-FUEL USES OF COALS AND SYNTHESIS OF CHEMICALS AND MATERIALS

Chunshan SONG and Harold H. SCHOBERT

Fuel Science Program, 209 Academic Projects Building,
The Pennsylvania State University, University Park, Pennsylvania 16802

Keywords: Non-fuel use, Coal, Chemicals, Materials

ABSTRACT

This paper provides an account of our analysis of future needs for non-fuel uses of fossil fuels, particularly coal, and a discussion of possible routes for developing chemicals and materials. An overview of energy supply and demand in the world and the existing non-fuel uses of fossil fuels in the U.S. will be given first. The amount of energy used for non-fuel purpose is small compared with the amount of energy consumed by end users. Nevertheless, the non-fuel uses of fossil fuels may become more important in the future. The demonstrated coal reserves in the world are enough for consumption of over 220 years at the 1992 level, while the oil reserves are only about 40 times of the world's consumption level in 1992. Coal may become more important both as energy source and as the source of chemical feedstocks as we move into the 21st century. However, traditional non-fuel uses of coals (coke ovens and the coal tars) are diminishing rapidly. We will discuss the possible new processes for making both bulk and specialty chemicals and polymers and carbon materials from coals and liquids from coal liquefaction. Specific examples will be provided from work in progress in our laboratory, including conversion of coals and coal liquids to specialty chemicals, polymer materials, activated carbons, graphitic carbons, and electrode materials.

WORLD AND U.S. SUPPLY AND DEMAND OF FOSSIL FUELS

Table 1 summarizes energy supply and demand in the world and in the U.S., and the U.S. primary energy input into the electric utilities. The energy statistics data in this paper were derived from several recent DOE/EIA reports [EIA AER, 1993; AEO, 1994; IEO, 1994; IPSO, 1994; MER, 1993; QCR, 1994]. Fossil fuels are the dominant sources of energies for modern societies as well as chemicals and synthetic organic materials.

Currently the world consumes 66.9 million barrels of oils per day (mbpd) and 24.34 billion barrels per year (136.3 quadrillion Btu/year). According to the most recent report, the estimated crude oil reserves in the world are 999.1 billion barrels, with 66.3% in the Middle East region but only about 2.4% in the U.S. The world is consuming petroleum at a very fast speed. The sum of all the petroleum reserves in world is only 41 times the consumption in 1992.

As of 1992, the sum of all the known natural gas reserves in the world is 4375.8 trillion cubic feet, with about 40% in the former Soviet Union and only 3.8% in the U.S. The world total consumption in 1992 reached 74.7 trillion cubic feet, which is equivalent to 74.3 quadrillion Btu. The known reserves in the world are about 59 times the consumption level in 1992.

The worldwide coal consumption in 1992 is 5001 million short tons (4535.9 million metric tons), which is equivalent to 88.9 quadrillion Btu. The world coal reserves are 1145.3 billion short tons (1038.5 billion metric tons), with about 23.1% in the U.S. The world coal reserves are over 225 times the consumption level in 1992. In particular, coal is the most abundant fossil hydrocarbon resource in the U.S., and the U.S. coal reserves (265.2 billion short tons) are about 300 times the current domestic annual consumption. Coal is expected to become more important in the future both as energy source and as the source of chemical feedstocks.

OVERVIEW OF NON-FUEL USES OF FOSSIL FUELS

Table 2 shows the amount of fossil hydrocarbon resources used for non-fuel purposes. Non-fuel use of fossil fuels in the U.S. is small compared with the amount of energy consumed as fuels by end users. As shown in Table 2, the non-fuel use of fossil resources is overwhelmingly the use of petroleum products, primarily petrochemical feedstocks, asphalt and road oil, petroleum coke, and liquefied petroleum gases. Non-fuel use of coal is dominated by the coal carbonization to make metallurgical coke. The non-fuel use of natural gas includes making synthesis gas, olefins, and carbon blacks. In 1992, the 5.84 quadrillion Btu consumed for non-fuel uses of fossil fuels (including coals for coke production) represented 7.1% of total energy consumption in the U.S. (82.42 quadrillion Btu). Non-fuel use of petroleum is 13.2% of petroleum consumed in the U.S.

Status of U.S. Coal Production and Utilization. Figure 1 shows the profile of the U.S. coal production by type over the period 1960-1992. Currently U.S. coal industry employs about 120 thousand miners, and produces about 1 billion short tons (about 900 million metric tons) of coals

annually [NCA, 1993]. About 90% of the coals are consumed domestically. About 10% of coals mined in the U.S. are exported, and they are bituminous coals, including about 43 and 60 million short tons of steam coals and metallurgical coals, respectively [NCA 1993].

As shown Table 3, electric utilities are the dominant consumers of coals. In fact, their consumption grew from 177 to 780 million tons during 1960-1992 [Song, Schobert, Scaroni, 1994]. The percentage distribution of the domestic consumption in 1992 is as follows: 87.2% by utilities, 8.4% by industries, 3.8% by coke plants, and 0.6% by residential and commercial users. Coal accounted for about 80 % of all the fossil fuels consumed at electric utilities in 1992.

Non-fuel Uses of Coals. Existing non-fuel uses of coals include (1) high temperature carbonization of bituminous coal to make metallurgical coke; (2) gasification of coal to make synthesis gases and other chemicals; (3) use of coal in manufacturing other materials such as activated carbons, carbon molecular sieves (CMS) and production of phosphoric acid; (4) the use of coal tars from carbonization (and gasification) for making aromatic chemicals; and (5) the use of coal tar pitch for making carbon fibers and activated carbon fibers, and other related products.

Energy Policy Act of 1992. Non-fuel uses of coals have also been described under the Section 1304 of the National Energy Policy Act of 1992: The Secretary of Energy shall plan and carry out a program of research, development, demonstration, and commercial application with respect to technologies for the non-fuel use of coal, including (1) production of coke and other carbon products derived from coal; (2) production of coal-derived, carbon-based chemical intermediates that are precursors of value-added chemicals and polymers; (3) production of chemical feedstocks via coal treatment processes.

Non-fuel Use through Coal Liquefaction. It is expected that coal liquefaction could become a viable option sometime in the next century, for producing liquid transportation fuels as well as chemical feedstocks. Despite enormous strides in coal liquefaction research and development, coal-derived liquid fuels are still not economically competitive with petroleum. However, the economic analysis of the viability of coal liquefaction may well produce a different result if some coal-derived liquids, particularly aromatic and phenolic compounds, can be used for making value-added chemicals and polymer materials. Just as crude oils are also used for making petrochemicals, the liquids from coal liquefaction are expected to provide the needed organic chemicals, albeit in smaller amounts compared to their use as fuels.

The importance of promoting non-fuel uses of coal in conjunction with coal liquefaction in the future is also apparent from the following facts. In 1970 the daily petroleum production and consumption in the U.S. were 9.64 and 14.70 million barrels, respectively. However, the U.S. petroleum production decreased to 6.84 million barrels/day in 1993, whereas the consumption increased to 17.03 million barrels/day. The worldwide petroleum consumption also rose from 46.81 million barrels/day in 1970 to 66.93 million barrels/day in 1993, which is a 43% increase in 22 years. Currently, the U.S. petroleum consumption is about 24.6% of the world's total consumption, but U.S.'s petroleum reserves are only about 2.4% of the world's total reserves. The remaining crude oils in the existing reserves are getting heavier. For example, the average API gravity of crudes refined in the U.S. decreased from 33.8 to 31.8 during the 10 years between 1980 and 1990; related to this increase in density (decrease in API gravity) is a constant rise in the sulfur content of the crude oils, from 0.88 wt% in 1980 to 1.11 wt% in 1990 [Swain, 1991]. With the continuing decline in the resource and in the quality of crude oils, the processing of coal-derived oils in existing petroleum refineries may become economically viable sometime in the 21st century.

Liquids from coal liquefaction may be used as feedstocks for making organic chemicals and various carbon materials, in addition to their use for producing transportation fuels. Relative to heavy oils, the problems associated with refining coal-derived liquids are their higher contents of aromatics, particularly polycyclic aromatics, and higher contents of nitrogen- and oxygen-containing compounds. Sulfur removal does not seem to be such a technical problem, since it is thought that hydrodesulfurization is easier, chemically, than hydrodenitrogenation. In the context of the production of chemicals and specialty materials, however, the high contents of aromatics, phenolics, and nitrogen compounds may provide a practical application of the folk adage, "If life hands you a lemon, make lemonade." If the "lemon" is the problem of dealing with the oxygen and nitrogen compounds prior to conventional refining for fuel use, the "lemonade" may be the use of these compounds and their derivatives for making value-added chemicals and monomers for aromatic polymer materials.

SYNTHESIS OF CHEMICALS AND POLYMERS FROM COALS

Before 1945 about 75% of all the organic chemicals in the world were based on coal-derived liquids, but with the advent of vast petroleum resources in the world during the 1940s, crude oil gradually became dominant chemical feedstocks by 1960. Currently petroleum and natural gas account for more than 90% of the major industrial organic chemicals [Speight, 1991; Sheldon, 1983]. These resources are the primary sources of the seven basic organic chemical building blocks: ethylene, propylene, butadiene, benzene, toluene, the xylenes, and methanol. However, coal tars remain an important source of aromatic chemicals. The annual consumption of aromatic chemicals worldwide is about 25 Mt for benzene, toluene, and xylenes; and 5 Mt for naphthalene and three- and four-ring compounds [Murakami, 1987; Collin, 1985]. Coal tar accounts for about 15-25% of the BTX production and 95% of the larger aromatics.

The last two decades have witnessed enormous developments in various organic and carbon-based materials [Song and Schobert, 1993], and it is certain that the late 1990's and the 21st century will see significant further growth of these materials. Examples include engineering plastics, liquid crystalline polymers, high-temperature heat-resistant polymers, polymer membranes, graphitic carbon materials, carbon fibers, and activated carbon fibers. Many of the starting materials for monomers of the aromatic polymer materials are not readily available from petroleum.

Scheme I shows some important aromatic polymer materials [Song and Schobert, 1993]. Scheme II gives the structures of some important liquid crystalline polymers [Song and Schobert, 1993]. Due to the recent development of many aromatic polymer materials, there is a great demand for aromatic monomers. Since the U.S. production of coal tar, which is an important source for 1- to 4-ring chemicals (particularly 2- to 4-ring aromatics), has declined significantly in the past decade, there is a need for developing an alternative source of aromatic chemicals in the future. With the rapidly increasing engineering applications of aromatic compounds for polymer materials, the demands for many aromatics of one to four rings have increased in the recent past, and this trend is expected to continue into the 21st century. Thus an excellent opportunity exists to explore the potentials of developing value-added chemicals and specialty materials from coals and the liquids obtained from coal liquefaction.

As we have discussed in detail elsewhere [Song and Schobert, 1993], research on deriving coal-based chemicals from coal liquids can be viewed as an extension of coal liquefaction research. Development of value-added chemical products could both increase the economic viability of coal liquefaction and make coal liquids more competitive with petroleum because coal liquids contain many compounds not found in petroleum [Song et al., 1991, 1992; Lai et al., 1992; Zhou et al., 1992; Saini and Song, 1994]. In analogous fashion, the economic viability of processing heavy residual materials could also be strengthened if approaches were developed for their conversion into value-added chemical feedstocks as well as transportation fuels.

We suggest that two broad approaches can be taken for coal conversion into value-added chemicals. The first can be viewed as the indirect approach, analogous to the so-called "indirect" coal-to-chemical conversion [Schobert, 1984]. The essence of the indirect approach would be the conversion of coals to liquids. Once the liquids were obtained, they would be subjected to appropriate separation or conversion operations to produce the chemical products of interest. However, separation of coal liquids into individual compounds is time consuming and expensive. An analogy from coal processing is the concept of combining short-contact-time liquefaction with catalytic dealkylation to produce aromatic hydrocarbon monomers [Song et al., 1989; Hirota et al., 1989]. The simplified aromatic compounds will then be used for making value-added products. The alternative, much bolder and of much higher risk, is the direct approach. In this approach a reagent would be introduced to the coals to cleave only a certain well-defined set of bonds and carefully cut out the molecular structures of interest. The highly selective removal of these structures could lead to monomers or precursors to the monomers for some of the high-performance polymer materials. An analogy proposed for direct production of chemicals from coal would be the use of selective oxidation to generate high yields of benzene carboxylic acids from low-rank coals [Song and Schobert, 1993].

On-going Research on Catalytic Synthesis of Chemicals in This Laboratory

In this section, specific examples will be provided from work in progress in our laboratory, including conversion of aromatic compounds in coal liquids to value-added chemicals, specialty chemicals, and monomers for polymer materials. We are exploring the catalysts, reactions, and processes for developing value-added chemicals and materials from coal-derived, carbon-based compounds.

Production of Phenol and Aromatics from Coals via Liquefaction. We are studying coal liquefaction in conjunction with the production of aromatic chemicals. Analysis of various coal-derived oils indicates that there are many 1- to 4-ring aromatic and polar compounds in coal-derived liquids that can be converted into valuable chemicals [Lai et al., 1992; Song and Schobert, 1993; Burgess et al., 1993; Huang et al., 1994; Saini and Song, 1994; Song and Saini, 1994; Lai and Song, 1995]. For example, phenol, naphthalene, and phenanthrene are rich in coal liquids from primary liquefaction of some coals. Phenol is one of the top twenty organic chemicals [CEN, 1994] and is commercially synthesized through multi-step process (benzene isopropylation, oxidation of isopropyl benzene, separation of phenol). However, phenol is rich in the oils from coal liquefaction, particularly when the liquefaction is promoted by dispersed catalysts and water [Song and Saini, 1994; Saini and Song, 1994]. Phenol can be separated directly from the coal liquids, and it can be used as or converted into monomer for many aromatic polymers and engineering plastics, including those shown in Scheme I. Naphthalene and its derivatives are rich in the oils from some bituminous coals. Naphthalene and 2-alkylnaphthalene are important aromatic chemicals. It should be noted that the use of aromatic compounds, that are in coal liquids and heavy oils, for making value-added chemicals requires the starting material to be reasonably pure. Our recent catalytic studies include the shape-selective conversion of two- to three-ring aromatic compounds (naphthalene, phenanthrene, and their derivatives) into value-added chemicals, as described below.

Shape-selective Alkylation of Naphthalene. This catalytic reaction can produce 2,6-dialkyl substituted naphthalene (2,6-DAN). 2,6-DAN is needed now as the feedstock of monomer for making the advanced polyester materials such as polyethylene naphthalate (PEN, Scheme I), polybutylene naphthalate (PBN, Scheme I), and liquid crystalline polymers (LCP, Scheme II). By using some shape-selective catalysts, we have achieved selective alkylation of naphthalene, with over 65% selectivity to 2,6-DAN by using isopropanol [Song and Kirby, 1993, 1994] or propylene as the alkylating agent [Schmitz and Song, 1994]. We also found some simple and effective methods for

enhancing the selectivity, which are not available in the prior arts [Schmitz and Song, 1994, unpublished data].

Ring-shift Isomerization of Phenanthrene Derivatives. This reaction leads to anthracene derivatives, particularly sym-octahydroanthracene (sym-OHAN). We have found that some catalysts selectively promotes the transformation of sym-octahydrophenanthrene into sym-OHAN, which we call ring-shift isomerization [Song and Moffat, 1993, 1994]. Some catalysts can afford over 90% selectivity with high conversion [Lai and Song, 1994, unpublished data]. This work could provide a cheap route to making anthracene and its derivatives, which are valuable chemicals in demand, from phenanthrene, which is rich in coal tar from coal carbonization, pyrolysis, and liquefaction. Examples of the possible applications of sym-OHAN may include the manufacturing of anthracene (which is in demand for making dyestuffs), anthraquinone (which is an effective pulping agent), and pyromellitic dianhydride (which is the monomer for making polyimides such as Du Pont's Kapton).

Conformational Isomerization of cis-Decalin to trans-Decalin. The commercial decalin solvents are almost equimolar mixtures of cis-decalin and trans-decalin. In an earlier work using decalin as a solvent, we found accidentally that cis-decalin isomerize into trans-decalin at low temperatures (250°C) over some catalysts [Song and Moffat, 1993, 1994], which would otherwise requires a high temperature such as 450°C [Song et al., 1992]. This work is a continuation of our earlier observation that trans-decalin has substantially higher thermal stability at high temperatures [Song et al., 1992]. Our recent experimental results indicate that it is possible to achieve over 90% conversion with 95% selectivity with some catalysts at low temperatures such as 200°C [Lai and Song, 1994, unpublished]. Possible application of this work is the manufacture of high-temperature heat-transfer fluids. Another application lies in the production of advanced thermally stable jet fuels, which can be used both as heat sinks and as fuels that are required for high-Mach aircraft [Schobert et al., 1994].

Shape-selective Naphthalene Hydrogenation. Complete hydrogenation of naphthalene in conventional process produce mixtures of cis- and trans-decalin, and . In recent studies on naphthalene hydrogenation, we have found that certain catalysts selectively promote the formation of cis-decalin or trans-decalin [Song and Grainne, 1993, unpublished data; Schmitz and Song, 1994, unpublished data]. Now we can selectively produce cis-decalin, with over 80% selectivity at 100% conversion [Schmitz and Song, 1994, unpublished data]. cis-Decalin may have potential industrial application as the starting material for making sebacic acid, which can be used for manufacturing Nylon 6,10 and softeners.

PRODUCTION OF CARBON MATERIALS FROM COALS

Carbon materials represent an important market for non-fuel applications of coal and coal-derived pitch materials. We have discussed the possibilities of developing various coal-based carbon materials recently [Song and Schobert, 1993] based on the materials listed in several reviews by Walker [1986, 1990] and by Marsh [1989, 1991]:

- Metallurgical cokes
- Molecular sieving carbons (MSC)
- Pitch-based carbon fibers
- Mesocarbon microbeads (MCMB)
- Mesophase-based carbon fibers
- Carbon fiber reinforced plastic
- Carbon whiskers or filament
- Graphite and graphite-based materials
- Diamond-like films
- Activated carbons
- Activated carbon fibers
- Carbon electrodes
- Carbon blacks
- Intercalation Materials
- Elastic carbons
- Composite materials
- Fullerenes or "bucky-balls"

Carbon-based Materials Made Directly from Coals. Currently the production of metallurgical coke is the largest non-fuel use of coals, primarily bituminous coals. It is estimated that about 500 million tonnes (metric tons) of coke are produced annually in the world [Mochida and Sakanishi, 1993]. China is one of the largest producers and consumers of coals and coke. In 1992, China produced 1204 million short tons of coals [EIA IEO, 1994]. About 10% of coals mined in China are used for making metallurgical coke [Guo, 1994].

Figure 2 shows the profile of the U.S. metallurgical coal consumption and coke production over the period 1950-1992. Coal consumption by the U.S. coke industry (and some other industrial sectors) trended downward since early 1970s. The reasons have been discussed in our previous review [Song and Schobert, 1993]. In 1993, the metallurgical coal consumption and coke production in the U.S. were 31.3 and 23.2 million short tons, respectively. The annual demand for coke in the U.S. is expected to further decrease to 18.7 million short tons by 2002 [Gilbert, 1993]. The decrease in coke production also means a decline in coal tar production, which could lead to the shortage of both aromatic chemicals, particularly 2- to 4-ring chemicals, and the pitch feedstocks for making carbon fibers and other needed carbon materials. This also gives rise to the need for developing alternate coal-based feedstocks for making various aromatic chemicals and carbon materials.

Activated carbons are used mainly as adsorbents for liquid-phase and gas-phase applications. In 1992, the world total annual production of activated carbons from various feedstocks was estimated

to be about 450,000 tonnes; among which 70,000 tonnes were produced in China, with about 30,000 tonnes made from coal and 40,000 tonnes from the other feedstocks [Gao, 1994]. The amount of coals used worldwide for producing activated carbons are estimated to be 200,000 tonnes/year [Golden, 1992]. Significant growth potential exists for this application, primarily for environmental protection, e.g., purification of water and air. Jagtoyen and Derbyshire have carried out a series of studies on the production of activated carbons from bituminous coals by chemical activation [Jagtoyen et al., 1992, 1993]. The liquid phase applications include water purification, decolorizing, food processing, and gold recovery, etc.; the gas phase applications cover air purification, gas treatment, and solvent recovery. More information on activated carbons may be found in a recent review by Derbyshire and co-workers [Derbyshire et al., 1994].

The amount of coals used worldwide for producing molecular sieving carbons are estimated to be 3,000 tonnes/year [Golden, 1992]. The application of molecular sieving carbons (MSC) for gas separation by pressure-swing adsorption (PSA) is now commercially viable. For example, MSC is used for air separation by Air Products and Chemicals Inc. It is expected that more companies will be engaged in producing MSC in the 1990's and into the next century.

The other industrial non-fuel uses of coals are included in those by industries and manufacturing plants, especially those who make chemicals, cement, paper, ceramics, and various metal products. Table 4 shows the U.S. coal consumption at manufacturing plants in 1992 by standard industrial classification (SIC) code [EIA QCR, 1994]. Use of coal for gasification can be partly classified as non-fuel use when the products are used as chemical feedstocks. Gasification is currently used for making synthesis gas ($\text{CO} + \text{H}_2$) and for producing H_2 for various hydrogenation and hydroprocessing in petrochemical and petroleum refining industries. The use of coal for gasification is included in Table 4 at the manufacturing plant with SIC code 29.

The details of the non-fuel uses at manufacturing plants are not available. However, direct coal injection into blast furnace is already in industrial practice. This use may have been included in SIC Code 33 in Table 4. There are some other interesting uses [Bonskowski, 1994]. Some lignite can be used as additive in drilling mud (drilling for oil and gas) as a lubricant and sealant. Young [1993] reviewed some other non-fuel applications of coals, particularly low-rank coals. They are 1) form coke from non-coking coals for use as a reductant in the metallurgical industries; 2) agricultural use of low-rank coals for production of coal-based fertilizers, soil conditioners, and humic acids; 3) special adsorbent carbons for storage of gases such as methane; and 4) production of carbon black and carbon support for making catalysts.

Carbon-based Materials Made from Coal-derived Liquids. The heavy fractions of coal tars, widely called coal tar pitches, are the raw materials for making carbon fibers and other carbon materials such as mesocarbon microbeads [Matsumura, 1989; Song and Schobert, 1993; Derbyshire et al., 1994].

The liquids and semi-liquids derived from coal extraction and liquefaction can also be used for making various carbon-based materials such as carbon fibers and graphitic materials. Kimber et al. [1981] and Zondlo et al. [1993] reported on the production of graphitic materials from carbonization of coal extracts. Kimber and Gray [1976] also noted that there are potential advantages in using coal-based coke for making carbon electrodes. Fei et al. [1994] reported on the production and properties of carbon fibers from coal-derived liquids as well as shale oils. Some lignite in California is used in an extraction process to make Montan wax, which may be used in shoe polishes, elastics, and electrical insulating [Bonskowski, 1994].

On-going Research on Production of Carbon Materials from Coal and Coal Liquids in This Laboratory

In the following section, specific examples will be provided from work in progress on carbon materials in our laboratory, including conversion of coal and pitch materials into various carbon materials.

Conversion of anthracite into graphite. Our interest in the possibility of converting anthracite into graphite was stimulated by two considerations: anthracites already contain well over 90% carbon, with aromaticities of essentially 1; and while anthracite currently sells in the range of \$80 per ton, the best quality graphite materials sell for about \$80 per pound. Our initial research was motivated by two hypotheses. First, the alignment of the large aromatic sheets presumed to exist in anthracite into the ideal graphitic structure could be facilitated by removing any residual heteroatom or aliphatic carbon atoms that might serve as covalent crosslinks "locking" the aromatic sheets into disordered structures. This, it was hypothesized, could be accomplished by reaction of anthracite with powerful hydrogen donors, such as 9,10-dihydrophenanthrene or 1,2,3,4-tetrahydro-fluoranthene prior to graphitization. Second, this process would be facilitated further if the spent donor (e.g., phenanthrene arising from 9,10-dihydrophenanthrene) was itself a graphitizable material and could therefore provide sites around which the graphitic structure could grow.

We have investigated the reactions of several Pennsylvania anthracites with hydrogen donors [Atria et al., 1993, 1994; Atria, 1995]. Co-carbonization of anthracite with a hydrogen donor, followed by high-temperature graphitization, produces a material having crystalline d-spacings in the range 0.3357–0.3361 nm, values which are quite close to the ideal value for graphite, 0.3354 nm. However, the crystalline height, L_c , of the best materials are in the range 54.7–58.8 nm, about half the value

(104.0 nm) observed in commercial graphite. As part of this work we have obtained unequivocal evidence that hydrogenation of anthracite does occur by direct reaction with hydrogen donors.

To further improve the quality of the graphitic product, we have begun an investigation of the catalytic graphitization of anthracites [Zeng et al., 1995a]. In this work, six Pennsylvania anthracites are being evaluated as feedstocks. The catalysts currently under investigation are La_2O_3 , Ce_2O_3 , and Gd_2O_3 , mixed with anthracites in amounts up to 5%. A second aim of this present project is to reduce substantially the temperature of graphitization. We are investigating graphitization temperatures as low as 1800°C, whereas in our earlier work much of the graphitization was done at 2900°C. A very large reduction in graphitization temperature translates to a significant energy saving in the graphitization process.

Conversion of Coals into Activated Carbons. At present, the main thrust of our work is again devoted to Pennsylvania anthracites. A small collateral effort is underway on activation of Turkish low-rank coals, in conjunction with various agricultural products indigenous to Turkey.

Steam and air activation have been investigated for production of carbons from anthracites [Gergova et al., 1993a, 1993b]. The highest BET surface area obtained was 720 m^2/g [Gergova et al., 1993b]. The particle size of the anthracite is a critical parameter; the best carbon (in terms of apparent surface area) was obtained from anthracite of <1 mm particle size. Subsequent work [Gergova et al., 1995] has used an environmental scanning electron microscope (ESEM) to observe development of a porous structure in real time, even though the ESEM operates at 2 Torr, whereas normally activation is done at atmospheric pressure. In this work we also investigated air treatment of the anthracite (e.g., 3 h at 300°C) prior to steam activation. The activated anthracites produced in the latter study have a microporous structure with a significant fraction of the pores having molecular dimensions. This suggests that molecular sieve materials could be produced from Pennsylvania anthracites.

Related Studies on Anthracites. Anthracite has long been an "orphan" in coal science research. Only a tiny fraction of the coal literature is devoted to reports of work on anthracites; in consequence, little fundamental information is available on anthracite properties and structure. Recently we have begun a collaborative effort with Carbone-Lorraine North America to investigate the basic physical properties of anthracites [Zeng et al., 1995b]. Major physical properties, including density, mechanical strength, hardness, coefficient of thermal expansion, and microstructure, are being measured and correlated with chemical properties such as proximate and ultimate analyses, porosity, apparent surface area, and aromaticity. The aim is to evaluate further the potentialities of using anthracites as raw materials for the production of various carbon products.

Very limited testing of the electrical properties of Pennsylvania anthracites has shown that they are not substantially below mesocarbon microbeads in some properties affecting use in lithium batteries or other dry cells [Zeng, 1994]. We infer, from this encouraging preliminary work, that limited, but controlled, structural modification of anthracites could make them attractive candidates for electrodes in batteries.

CONCLUDING REMARKS

Despite the relatively small amount of their non-fuel use, research into efficient use of the valuable hydrocarbon resources such as coal for non-fuel applications is becoming important.

We must always bear in mind that coal is an important source of hydrocarbons. There are many ways of using the hydrocarbon resources. Burning is only one of them. Expansion of the non-fuel uses is desirable, because coal will also become more important as source of both energy and chemical feedstocks in the next century. From the viewpoints of the resource conservation and effective utilization, many of the components in coals as well as in petroleum should be converted to, or used as value-added chemicals, polymers, and carbon materials.

George A. Olah, the 1994 Nobel Prize winner, pointed out recently [1991] that "oil and gas resources under the most optimistic scenarios won't last much longer than through the next century. Coal reserves are more abundant, but are also limited. ... I suggest we should worry much more about our limited and diminishing fossil resources." James L. Adams indicated in his recent book [1991] that "oil and coal used as fuel have allowed us to work wonders, but they are too valuable as complex hydrocarbons that can be converted into all sorts of the forms (such as plastics) to be so rapidly burned in automobiles, power plants, and furnaces."

ACKNOWLEDGMENTS

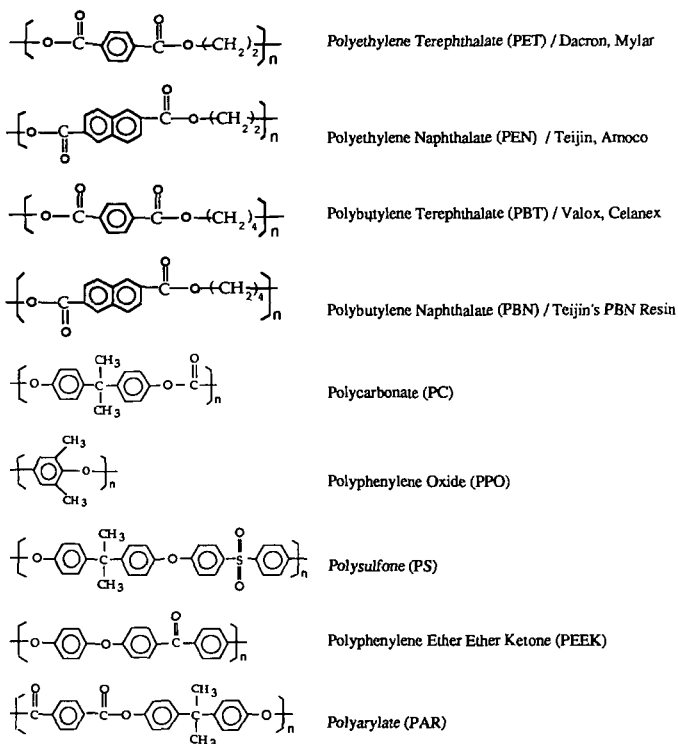
Various portions of our research were supported through funding or donations of special samples from the U.S. Department of Energy, Pittsburgh Energy Technology Center, Pennsylvania Energy Development Authority, Air Products and Chemicals Inc., PQ Co, and Duracell Co. Helpful discussions with Professor H. Marsh of Southern Illinois University, Dr. T. Golden of Air Products and Chemicals Inc., Dr. G.M. Kimber of British Coal Co., Dr. K.C. Krupinski of Aristech Chemical Co., Dr. R. F. Bonskowski of DOE/EIA, Dr. J. Broadhead of Duracell Worldwide Technology Center, and Drs. F. Rusinko, S. Eser, S. Zeng, W.-C. Lai, and A. Schmitz of PSU are gratefully acknowledged.

REFERENCES

- Adams, J. L. *Flying Buttresses, Entropy, and O-Rings. The World of an Engineer.* Harvard University Press, 1991, p.241.
- Atria, J. S.M. Zeng, H.H. Schobert, and F. Rusinko, Jr. A novel approach to the production of graphite from anthracite, *Proceedings 21st Biennial Conference on Carbon*, pp. 342-343, 1993.
- Atria, J.V., S. Zeng, F. Rusinko, Jr., and H.H. Schobert. Novel approach to the production of graphite from anthracite. *Am. Chem. Soc. Div. Fuel Chem. Prepr.*, 1994, 39, 884-888.
- Atria, J.V. Production of anthracite from graphite, M.S. Thesis, The Pennsylvania State University, University Park, PA, 1995.
- Bonskowski, R. F. Energy Information Administration, U.S. DOE. personal communication. November 9, 1994.
- Burgess, C. E., K. Wenzel, C. Song, P. G. Hatcher, and H. H. Schobert. Structural Correlation of Coal Liquefaction Oils with Flash Pyrolysis Products. *Proc. 7th Internat. Conf. Coal Sci., Banff Canada*, Sept. 12-17, 1993, Vol. 1, pp.311-314.
- CEN *Chem. Eng. News*, July 4, 1994
- Collin, G. Erdol und Kohle - Erdgas Petrochem. 1985, 38 (11), 489-496
- Derbyshire, F. J., M. Jagtoyen, Y. Q. Fei, and G. Kimber. *Am. Chem. Soc. Div. Fuel Chem. Prepr.*, 1994, 39 (1), 113-120.
- Energy Information Administration (EIA). Annual Energy Review (AER) 1992, U.S. DOE, Report No. DOE/EIA-0384(92), June 1993.
- EIA AEO Annual Energy Outlook 1994, DOE/EIA-0383(94), January 1994.
- EIA IEO International Energy Outlook (IEO), DOE/EIA-0484(94), July 1994.
- EIA IPSR International Petroleum Statistics Report (IPSR), DOE/EIA-0520(94/04), April 1994.
- EIA MER Monthly Energy Review (MER), DOE/EIA-0035(93/08), August 1993.
- EIA QCR Quarterly Coal Report (QCR), July-September 1993, DOE/EIA-0121(93/3Q), February 1994.
- EIA QCR Quarterly Coal Report (QCR), January-March 1994, DOE/EIA-0121(94/1Q), August 1994.
- Fei, Y.Q., F. Derbyshire, M. Jagtoyen, and I. Mochida. Advantages of Producing Carbon Fibers and Activated Carbon Fibers from Shale Oils. *Proc. of 1993 Eastern Oil Shale Sym.*, May 1994.
- Gao, S. Activated Carbon Industry in China. *Tanso (Japanese)*, 1994, No. 163, 145-149.
- Gergova, K., S. Eser, and H.H. Schobert. Pyrolysis/activation of anthracite for production of activated carbons, *Proceedings, 21st Biennial Conference on Carbon*, pp. 412-413, 1993.
- Gergova, K., S. Eser, and H.H. Schobert. Preparation and characterization of activated carbons from anthracite. *Energy and Fuels*, 1993, 7, 661-668.
- Gergova, K., S. Eser, H.H. Schobert, M. Klimkiewicz, and P.W. Brown. Environmental scanning electron microscopy of producing activated carbons from anthracite using one-step pyrolysis/activation. *Fuel*, 1995, in press.
- Gilbert, B.R. Co-production of Iron and Methanol. *Proc. 10th Ann. Internat. Pittsburgh Coal Conf., University of Pittsburgh, Pittsburgh*, Sept. 20-24, pp.410-415, 1993.
- Golden, T.C. Air Products Co., personal communication, April 24, 1992.
- Guo, S. Present State and Overview of Coal Utilization Technology in China. *Energy & Resources (Japanese)*, 1994, 15 (2), 161-165.
- Hirota, T., M. Nomura, and C. Song. A Method for Manufacture of Aromatic Chemicals from Coals. *Japan Patent*, 1-279990 (Assigned to Osaka Gas Company, Japan), November 10, 1989 (in Japanese).
- Huang, L., C. Song, and H. H. Schobert. Liquefaction of Low-Rank Coals as a Potential Source of Specialty Chemicals. *Am. Chem. Soc. Div. Fuel Chem. Prepr.*, 1994, 39 (2), 591-595.
- Jagtoyen, M., M. Thwaites, J. Stencil, B. McEnaney, and F. Derbyshire. Adsorbent Carbon Synthesis from Coals by Phosphoric Acid Activation. *Carbon*, 1992, 30 (7), 1089-1096.
- Jagtoyen, J. Groppo, and F. Derbyshire. Activated Carbons from Bituminous Coals by Reaction with H3PO4: The Influence of Coal Cleaning. *Fuel Process. Technol.*, 1993, 34, 85-96.
- Kimber, G. M., and M. D. Gray. Comparison of Evolution of Heteroatoms from Coal and Petroleum Based Electrode Cokes. *Am. Chem. Soc. Sym. Ser.*, 1976, 21, 445-450.
- Kimber, G. M., A. Brown, and J. N. Kirk. Arc-steel Electrodes from Coal via Solvent Extraction. *High Temp. - High Press.*, 1981, 13, 133-137.
- Lai, W.-C., C. Song, H. H. Schobert., and R. Arumugam. Pyrolytic Degradation of Coal- and Petroleum-Derived Aviation Jet Fuels and Middle Distillates. *Am. Chem. Soc. Div. Fuel Chem. Prepr.*, 1992, 37 (4), 1671-1680.
- Lai W.-C. and C. Song, 1994, unpublished data, The Pennsylvania State University.
- Lai, W.-C. and C. Song. Temperature-Programmed Retention Indices for GC and GC-MS Analysis of Coal- and Petroleum-derived Liquid Fuels. *Fuel*, to be published, 1995.
- Marsh, H. 1991. "New and Traditional Carbon Materials from Petroleum and Coal Sources". Paper presented at Information Transfer Session, Cooperative Program in Coal Research, November 18-19, Pennsylvania State University, University Park, PA.
- Marsh, H. (Ed.), 1989. "Introduction to Carbon Science", Butterworths, London, 321 pp.
- Matsumura, Y. Current Status and Perspectives of Coal Pitch-Based Carbon Fibers. *Kagaku Keizai (Japanese)*, 1989a, No.9, 33-41
- Matsumura, Y. Expanding Applications of Pitch-Based Carbon Materials. *JETI (Japanese)*, 1989b, 37 (No.9), 223-226.
- Mochida, I. and K. Sakanishi. Tasks and Scopes of Coal Science. *J. Japan Inst. Energy (Japanese)*, 1993, 72 (5), 312-320.
- Murakami, H. *Nenryo Kyokai-Shi (Japanese)*, 1987, 66 (6), 448-458.
- NCA Facts about Coal. National Coal Association, July 1993.

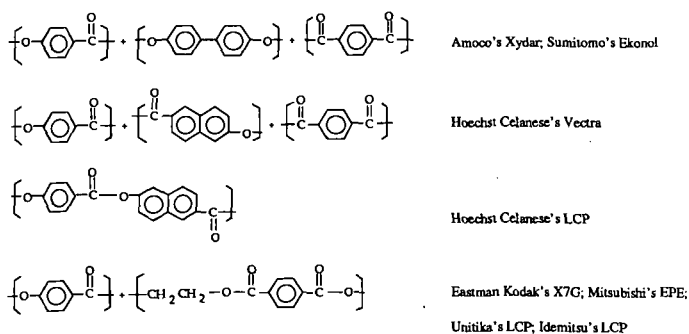
- Olah, G. A. Nonrenewable Fossil Fuels. Chem. Eng. News, February 11, 1991.
- Saini, A. K., and C. Song. Two-Dimensional HPLC and GC-MS of Oils from Catalytic Coal Liquefaction. Am. Chem. Soc. Div. Fuel Chem. Prepr., 1994, 39 (3), 796-800.
- Schmidt, E., and C. Song. Model Hydrocracking Reactions over Monometallic and Bimetallic Dispersed Catalysts. Am. Chem. Soc. Div. Fuel Chem. Prepr., 1994, 39 (3), 733-737.
- Schmitz, A., and C. Song. Shape-Selective Isopropylation of Naphthalene over Dealuminated Mordenite. Am. Chem. Soc. Div. Fuel Chem. Prepr., 1994, 39 (4), 986-991.
- Schmitz and Song, 1994, unpublished data, The Pennsylvania State University.
- Schobert, H.H., 1984. In: W.R. Kube, E.A. Sondreal, and C.D. Rao (Eds.), Technology and Utilization of Low-rank Coals. U.S. Dept. of Energy Report DOE/METC/84-13; pp. 83-103.
- Schobert, H.H., S. Eser, C. Song, P. G. Hatcher, P. M. Walsh, and M. M. Coleman. Advanced Thermally Stable Jet Fuels. Technical Report, U.S. Department of Energy, DE-FG22-92PC92104-TPR-8, July 1994, 96 pp.
- Sheldon, R.A. Chemicals from Synthesis Gas. Reidel Pub. Co., Boston, 1983
- Song, C., K. Hanaoka, and M. Nomura. Short-Contact-Time Pyrolytic Liquefaction of Wandoan Subbituminous Coal and Catalytic Upgrading of SCT-SRC. Fuel, 1989, 68 (3), 287-292.
- Song, C. and H. H. Schobert. Specialty Chemicals and Advanced Materials from Coals: Research Needs and Opportunities. Am. Chem. Soc. Div. Fuel Chem. Prepr., 1992, 37 (2), 524-532.
- Song, C. and S. Kirby. Shape-Selective Alkylation of Naphthalene over Molecular Sieve Catalysts. Am. Chem. Soc. Div. Petrol. Chem. Prepr., 1993, 38 (4), 784-787.
- Song, C. and K. Moffatt. Zeolite-Catalyzed Ring-Shift and Conformational Isomerization Reactions of Polycyclic Hydrocarbons. Am. Chem. Soc. Div. Petrol. Chem. Prepr., 1993, 38 (4), 779-783.
- Song, C. and H. H. Schobert. Opportunities for Developing Specialty Chemicals and Advanced Materials from Coals. Fuel Processing Technol., 1993, 34 (2), 157-196.
- Song, C. and H. H. Schobert. Aromatic Polymer Precursors from Coals: A New Direction in Coal Chemistry. Proc. 10th Ann. Internat. Pittsburgh Coal Conf., University of Pittsburgh, Pittsburgh, Sept. 20-24, pp.384-389, 1993.
- Song, C. and S. Kirby. Shape-Selective Alkylation of Naphthalene with Isopropanol over Mordenite Catalysts. Microporous Materials, Elsevier, 1994, 2 (5), 467-476.
- Song, C. and K. Moffatt. Zeolite-Catalyzed Ring-Shift Isomerization of sym-Octahydrophenanthrene and Conformational Isomerization of cis-Decahydronaphthalene. Microporous Materials, Elsevier, 1994, 2 (5), 459-466.
- Song, C., H.H. Schobert, and A.W. Scaroni. Current Status of U.S. Coal Utilization Technologies and Prospects. Energy & Resources (Japanese), 1994, 15 (2), 142-153.
- Song, C., and A. K. Saini. Using Water and Dispersed MoS₂ Catalyst for Coal Conversion into Fuels and Chemicals. Am. Chem. Soc. Div. Fuel Chem. Prepr., 1994, 39 (4), 1103-1107.
- Speight, J.G. (Ed.), Fuel Science and Technology Handbook. Marcel Dekker: New York, 1990, 1193 pp.
- Speight, J.G., The Chemistry and Technology of Petroleum. Marcel Dekker: New York, 1991, Chapter 21 (Petrochemicals), p.717.
- Swain, E.J. U.S. Crude Slate Gets Heavier, Higher in Sulfur. Oil Gas J., 1991, September issue, 59-61.
- Walker, P.L., Jr. 1986. Review Article: Coal Derived Carbons. Carbon, 24 (4): 379-386.
- Walker, P.L., Jr. 1990. Carbon: An Old but New Material Revisited. Carbon, 28: 261-279.
- Young, B.C. Meeting the Value-Added Challenge with Coal Briquetting and Pelleting. Proc. 10th Ann. Internat. Pittsburgh Coal Conf., University of Pittsburgh, Pittsburgh, Sept. 20-24, pp.402-407, 1993.
- Zeng, S. Unpublished data, The Pennsylvania State University, University Park, PA, 1994.
- Zeng, S., F. Rusinko, Jr., H.H. Schobert, D.P. Struble, and W.A. Nystrom. Graphitization of anthracites with the addition of rare earth compounds. Proceedings, 22d Biennial Conference on Carbon, (submitted, 1995).
- Zeng, S., F. Rusinko, Jr., H.H. Schobert, D.P. Struble, and W.A. Nystrom. Investigation of the physical properties of Pennsylvania anthracites. Proceedings, 22d Biennial Conference on Carbon, (submitted, 1995).
- Zhou, P.-Z., Marano, J.J. and Winschel, R.A., 1992. Prepr. Pap.-Am. Chem. Soc., Div. Fuel Chem., 37 (4), 1847-1854.
- Zondlo, J.W., P.G. Stansberry, and A.H. Stiller. Pitch and Coke Production via Solvent Extraction of Coal. Proc. 10th Ann. Internat. Pittsburgh Coal Conf., University of Pittsburgh, Pittsburgh, Sept. 20-24, pp.379-383, 1993.

Scheme I. Structures of Some Important Aromatic Plastics Materials



Scheme II. Structures of Some Important Liquid Crystalline Polymers (LCPs)

Thermotropic Polyester LCPs



Lytropic LCP



Table 1. World and U.S. Energy Supply and Demand

Year	Total	Petroleum	N. Gas	Coal	Nuclear	Hydropower	Other
World Total Energy Consumption / Quadrillion Btu (10^{15} Btu)							
1992	347.5	136.3	74.3	88.9	21.5	22.3	4.4
U.S. Energy Consumption / Quadrillion Btu							
1992	82.42	33.51	20.34	18.89	6.65	2.81	0.22
U.S. Energy Production / Quadrillion Btu							
1992	66.93	15.22	20.67	21.68	6.65	2.81	0.22
U.S. Energy Input at Electric Utilities / Quadrillion Btu							
1992	29.56	0.95	2.83	16.19	6.65	2.76	0.19

Note: According to DOE EIA, 1 quadrillion Btu is equivalent to 45 million short tons of coal, 170 million barrels of crude oil, and 1 trillion cubic feet of dry natural gas.

Table 2. Non-fuel Use of Fossil Fuels in the U.S. in 1992

Coal		Petroleum							N. Gas	
Coke	Other	Petro-chemical feedstocks	Asphalt and Road Oil	Liquefied Petroleum Gases	Lubricant	Petroleum Coke	Special naphtha	Wax, etc.	Chemical feedstocks	
Physical Unit / million short tons for coal; million barrels for oil; billion cubic feet for natural gas										
32.37	1.8	202	166	386	54	42	19	27	611	
Energy Unit / Quadrillion Btu (10^{15} Btu)										
0.73	0.05	1.14	1.10	1.35	0.33	0.25	0.10	0.16	0.63	

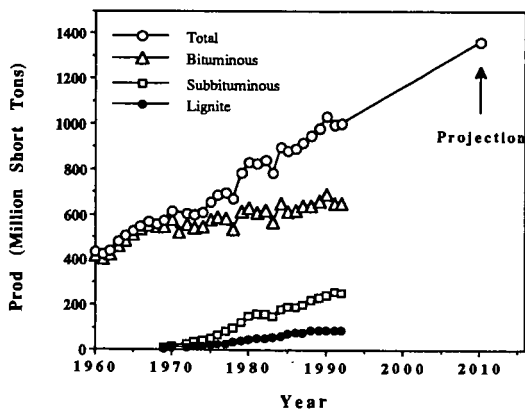


Figure 1. Production of coal by type in the U.S. during 1960-1992 (1 short ton = 0.907 metric ton).

Table 3. U.S. Coal Production and Consumption

Coal Supply and Demand / million short tons					
Year	Production	Consumption	Export	Import	Others and losses
1992	997.545	892.421	102.516	3.803	9.407

Coal Consumption by Sectors / million short tons					
Year	Electric Utilities	Coke Plants	Other Industrial	Residential and Commercial	Total consum.
1992	779.860	32.366	74.042	6.153	892.421

Note: 1 short ton = 907.184 kg = 2000 pounds = 0.907 metric ton

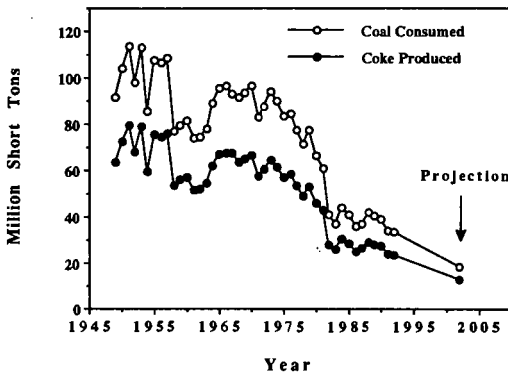


Figure 2. U.S. metallurgical coke production during 1949-1992

Table 4. U.S. Coal Consumption at Manufacturing Plants by Standard Industrial Classification Code (Thousand Short Tons)

SIC Code	Jan-March	Apr-June	July-Sept	Oct-Dec	U.S. Total
	1993	1993	1993	1993	
20 Food and kindred products	2264	1568	1491	2479	7802
21 Tobacco products	184	156	154	154	648
22 Textile mill products	370	313	258	334	1275
24 Lumber and wood products	27	29	23	30	109
25 Furniture and fixtures	35	18	16	32	101
26 Paper and allied products	3302	2918	2946	3270	12436
28 Chemicals, allied products	3490	3079	3044	3338	12951
29 Petroleum and coal products ¹	1760	1832	1695	1963	7250
30 Rubber, misc. plastics products	78	67	56	64	265
32 Stone, clay, glass products	2781	3170	3329	3478	12758
33 Primary metal industries ²	1623	1833	1700	1872	7028
34 Fabricated metal products	113	59	33	80	285
35 Machinery, except electric	180	84	48	121	433
36 Electric, electronic equipment	89	59	29	68	245
XX Other manufacturing industries (SIC: 23, 27, 31, 37, 38, 39)	w	w	w	w	w
U.S. Total	17175	15705	15268	17931	66079

1) Includes coal gasification projects.

2) Excluding coke plants. w Withheld by DOE to avoid disclosure of individual company data.

PROCESSING, STRUCTURE AND PROPERTIES OF PITCH-BASED CARBON-CARBON COMPOSITES

S. P. Appleyard, B. Rand and C. E. Ahearn
School of Materials, University of Leeds,
Leeds, LS2 9JT, U.K.

Keywords: Carbon-carbon composite, pitch, fibre-matrix interface

INTRODUCTION

The potential of carbon-carbon (CC) composites as materials for high temperature applications was recognised at a very early stage, leading to their development in the 1960's as materials for thermal protection during space vehicle re-entry. By the early 1970's, two basic approaches to the formation of the carbon matrix were established, namely through chemical vapour deposition from a hydrocarbon gas (CVD) (1) and through carbonisation of a carbon-bearing resin or pitch (2). Fundamentally, little has changed since those early years with respect to these basic methods of CC composite fabrication. Further developments have, however, involved the introduction of multidirectional fibre architectures in order to reduce the mechanical anisotropy present in unidirectionally and bidirectionally reinforced composites caused by poor mechanical properties in the unreinforced directions. The strategic importance of several aerospace applications of CC composites, including military rocket nozzles and nose cones, the NASA space shuttle nose cone and leading edge protection surfaces, aircraft brake discs and gas diverter fins, ensured their continued development during the 1970's and 1980's.

The technique of liquid impregnation is now a major procedure for the densification of CC composites (3). Despite nearly 30 years of development, however, the utilisation of fibre strength in densified CC composites is still only around 65 % (3). There is, therefore, a need for a comprehensive understanding of the factors giving rise to this lost potential so that improvements in properties may be achieved. Furthermore, new applications of CC composites are currently emerging which exploit some of the thermal characteristics of the composite structure as manifest in the graphite crystal structure. There is thus a need to further understand the ways in which the composite microstructure may be controlled during the fabrication process. This paper reviews the principal microstructural features of interest in CC composites produced with pitch precursors to the carbon matrix and illustrates the influence of fibre-matrix interactions on the microstructure and properties.

MICROSTRUCTURE OF CC COMPOSITES

The microstructures of CC composites may be very complex, involving various degrees of crystallinity and texture on differing scales of magnitude, and several types of interfaces, pores and microcracks, conceivably all in the same specimen (4). Both fibre and matrix undergo significant microstructural changes during fabrication; the fibre and matrix may interact, thus producing unique microstructural features that cannot be obtained by identical processing of the separate constituents (5).

The orientation of the outer turbostratic sheath of carbon fibres has been observed to increase on graphitisation compared with that of a fibre graphitised independently of a composite (6). This increased alignment is thought to arise from an interfacial stress effect. Fibres may thus undergo a substantial increase in modulus of elasticity during thermal processing of a CC composite (7). Such stresses, caused by strong fibre-matrix coupling and matrix shrinkage during carbonisation of the composite, have also been claimed to damage the fibre (8).

Although the overall texture of CC composites is dominated by the structure and architecture of the fibre reinforcement, the existence of preferred orientation (texture) in the microstructure of the matrix is significant. Texture in the matrix is established primarily from two sources, namely the chemistry of the organic matrix precursor and fibre-matrix interfacial effects. Matrix carbons derived from pitches tend to be structurally anisotropic, a product of the development of layers during the growth and coalescence of mesophase spheres in the initial stages of pyrolysis. If unhindered and mechanically undisturbed, the coalesced mesophase produces a coarse microstructure (9). Plastic deformation during this stage, due to externally applied stresses or the formation of gaseous by-products of pyrolysis, may disrupt long range ordering of the mesophase resulting in a finer microstructure. Similar effects are caused either by the application of pressure during carbonisation or by

chemical cross-linking of the structure (10, 11). Controlled alteration of the matrix microstructure may be achieved by the blending of various fractions of pitches (12).

Texture has been observed to initiate in previously structurally isotropic matrices on heat treatment to graphitising temperatures (13). This effect has been ascribed to a concentration of stress developing along the fibre-matrix interface, arising from the combined actions of matrix densification (volume shrinkage) and thermal expansion mismatch between the fibre and the matrix. A second form of fibre-matrix interfacial effect, characteristic of structurally anisotropic matrices, involves the development of carbon atoms arranged in planar layers oriented parallel to the fibre surface (14). A full understanding of this effect has not been reached. The "matrix sheath" may result from fluid flow rather than from wetting (15), though forces acting on the disc-like molecules by the surface do produce a strong anchoring effect, as detected by the resistance to orientation induced by a magnetic field (16). Disruption of the sheath can be produced by the application of pressure during carbonisation and the effects of chemical cross-linking of the structure (10, 11). Given the potential anisotropy in properties conferred by the structure of graphite, the ability to control the texture of the matrix is clearly important in order to allow complete control over the properties of the composite.

Graphitisation of anisotropic matrix carbons causes further structural changes to occur. These changes include "fold-sharpening" and "polygonisation". The former appearing to constitute the first point at which the process of graphitisation becomes microscopically evident (17); shrinkage cracking tends to break a sheet or fold into segments at fairly regular intervals, and these segments sharpen to decreasing radii of curvature. Polygonisation is evidenced by the formation of mosaic block type structures, and has the effect of relaxing the compressive stresses generated by the tendency to shear the layers into graphitic registry (17).

Few studies have been reported concerning the characterisation of porosity in CC composites. Jortner (18) distinguishes between "pores" and "cracks". Pores primarily arise from processing problems. Examples of these include pores formed by incomplete filling by the matrix (perhaps due to poor wetting of the fibres, or incomplete compaction of prepregs resulting in dry zones within the composite) and by the entrapment of gases produced during solvent removal, curing or pyrolysis while a matrix precursor is still liquid or plastic (18). Cracks, comprising "shrinkage", "cooldown" and "thermal stress heating" cracks, arise from stresses due to structural rearrangements during heat treatment or thermomechanical effects.

The geometry of the fibre architecture and nature of fabrication of CC composites generate a number of interfaces present on both the "mini-mechanical" and "micro-mechanical" scales (18). Interfaces that occur on the mini-mechanical scale include fibre tow-fibre tow, bundle-bundle, bundle-matrix and layer-layer interfaces. On the micro-mechanical scale exist fibre-matrix and matrix-matrix interfaces (18). The strength of the fibre-matrix interface is critical to the behaviour of CC composites under mechanical loading. A good fibre-matrix coupling is required to maximise energy transfer from the matrix to the fibre, though it must not be so strong as to cause brittle failure of the composite (19). Matrix-matrix interfaces also have importance as they may limit the ability of the matrix to distribute the load equally between fibre-matrix units or to redistribute the load around individual unit failures (20). In pitch-based carbon matrix composites, the structure of the interfacial zone is monopolised by the presence of matrix sheath, described above. This sheath may actually be a source of debonding of the interface due to the actions of fold-sharpening and polygonisation during graphitisation (11).

The exact nature of "bonding" at the interfaces in CC composites, and hence what controls the bond strength, is not fully understood. Various types of interaction across the interface may exist, including strong and weak chemical bonds, mechanical interlocking and friction (4). Full characterisation and control of interfaces remains one of the most elusive aspects of the technology of CC composites.

EXPERIMENTAL

Model unidirectional CC composites comprising continuous PAN-based fibres and petroleum pitch-based matrices were fabricated by wet-winding and moulding in a heated press, followed by heat treatment. Several types of PAN fibre were used. These included a surface treated standard modulus fibre (SMS) and an untreated high modulus fibre (HMU). Two main temperatures were chosen for the routine

heat treatment of composites. These were a "carbonisation" temperature of 900 °C and a "graphitisation" temperature of 2250 °C. The porous composites so formed were densified by means of pitch-melt impregnation. Composites were studied by optical and scanning electron microscopy and X-ray diffraction. Various properties were studied including electrical resistivity and mechanical behaviour.

STRUCTURAL AND PHYSICAL CHARACTERISATION

A major characteristic of the initial establishment of CC composite structures during carbonisation and graphitisation was the creation of a large number of voids due to matrix shrinkage. After initial carbonisation of the HMU-pitch composites, point counting revealed only ~ 20 % of the fibre surface to be contiguous with matrix. Cracks had developed which were mainly located at the fibre-matrix interface. These cracks, however, were extensively interconnected and enabled very efficient densification of the structure by pitch-melt impregnation. Cracks in the SMS composite, conversely, were generally located within the matrix and tended to have a thin lath-like morphology. This reflected the greater strength of the fibre-matrix interface due to the surface treatment of the fibre, and also revealed the matrix to be prone to failure due to cleavage of the anisotropic structure along planes of weakness. Densification of the SMS composites was not very efficient due to the "bottle-shape" nature of the voids. The location of shrinkage cracks was thus strongly influenced by the combination of the fibre-matrix interface strength and the strength and texture of the matrix (Figure 1). In turn, the void shapes and their degree of interconnectivity governed the efficiency of densification by liquid impregnation.

X-ray diffraction (002) profiles of the green and carbonised composites were largely dominated by the fibre (002) profiles. On graphitisation, marked changes in the composite (002) profiles occurred as they became matrix dominated. Deconvolution of the (002) intensity profiles into separate fibre and matrix profiles enabled $d_{(002)}$ and L_c to be determined for each constituent (Figure 2). The matrix L_c values were greater with respect to similarly heat treated bulk raw materials, indicating the effects on structure of fibre-matrix interactions during graphitisation.

Measurements of electrical resistivity were made both parallel and perpendicular to the fibre axes. Of the densified composites, the carbonised SMS composites exhibited the lowest electrical anisotropy (~ 6). This reflected both the lower structural anisotropy of the SMS fibre and matrix structures (cf. graphitised fibres / matrices) and the high degree of fibre-matrix contiguity present in the composite. Departures from one or more of these conditions resulted in greater anisotropy. Matrix resistivity in the axial direction was calculated by considering the composite as a sequence of parallel resistors, together with knowledge of the longitudinal fibre resistivities, V_f , V_m and V_c . The carbonised matrix resistivity averaged $1.64 \times 10^{-6} \Omega m$, reducing to $4.02 \times 10^{-6} \Omega m$ on graphitisation. The axial resistivity of the graphitised pitch matrix thus approximately matched that of highly oriented Amoco P-100 pitch-based fibres after individual heat treatment to 2500 °C (21). These measurements clearly illustrate the potential of the matrix sheath regarding control of composite properties; alignment of matrix carbon basal planes parallel to the fibre axis greatly enhanced composite electrical conductivity in the longitudinal direction.

MECHANICAL PROPERTIES

Flexural strengths were measured at span-to-depth ratios of 80:1. The strength of the fibre-matrix interface strongly influenced the mode of fracture during flexural testing. A range of fracture behaviour was observed, from "brittle-catastrophic" to "pseudo-ductile", depending on the fibre-matrix combination and fabrication history. The carbonised SMS composites failed by a brittle failure mechanism; only 25 % of the fibre strength was utilised. Failure of the carbonised, densified HMU composite was evidently by means of multiple matrix cracking followed by fibre failure and fibre pull-out. In this case 60 % utilisation of fibre strength was achieved (assuming the contribution of the matrix to strength to be negligible). Graphitisation may give rise to changes in the mode-of-failure due to changes in the nature of the interface and matrix texture. Similarly, low temperature oxidation, in which the oxidation reaction clearly takes place preferentially at the fibre-matrix interface may weaken the fibre-matrix interface enabling debonding and fibre sliding. Increases in utilisation of fibre strength may thus occur as a result of the greater strains at which maximum load occurs.

CONCLUSION

Successful control of fibre-matrix interactions at each stage of fabrication is key to the control of properties of CC composites. The void network established during the initial heat carbonisation has a large effect on the efficiency and effectiveness of subsequent densification processing. The influence of matrix texture on the electrical properties of CC has been illustrated; as the lattice properties of anisotropic carbons are similarly reflected in the properties of modulus of elasticity, thermal expansivity and thermal conductivity, an ability to control matrix texture is clearly of great importance. These properties are of especial importance regarding an emerging application of CC composites, namely the packaging of electronic systems. Finally, if improvements in utilisation of fibre properties are to be achieved, it is imperative to advance understanding of the various structural features influencing modes-of-failure.

REFERENCES

1. H. M. Stoller and E. R. Frye, Symposium of the 73rd Annual Meeting of the American Ceramic Society, *Advanced Materials: Composites and Carbon*, American Ceramic Society (1973) p163.
2. A. R. Taverna and L. E. McAllister, *ibid.* p199.
3. R. A. Meyer, *Materially Speaking* (Publication of The Materials Technology Centre, Southern Illinois University at Carbondale) **9**, Summer (1994) p1.
4. L. H. Peebles Jr., R. A. Meyer and J. Jortner, Proc. of 2nd Int. Conf. on Composite Interfaces, American Society of Metals, Ohio, Published as *Interfaces in Polymer, Ceramic and Metal Matrix Composites*, Ed. H. Ishida, Pub. Elsevier, New York (1988) p1.
5. R. J. Diefendorf, Extended Abstracts of the 13th Biennial Conference on Carbon, American Carbon Society, Irvine (1977) p381.
6. W. Kowbel, E. Hippo and N. Murdie, *Carbon* **27** (1989) p219.
7. R. Bacon, L. C. Nelson, S. L. Strong, E. F. Valla and G. Wagoner, Extended Abstracts of the 19th Biennial Conference on Carbon, American Carbon Society, Penn State (1989) p342.
8. E. Fitzer and A. Bürger, Proc. 1st Int. Conf. on Carbon Fibres, The Plastics Institute, London (1971) p134.
9. J. E. Zimmer and J. L. White, Disclination Structures in the Carbonaceous Mesophase in *Advances in Liquid Crystals* **5**, Pub. Academic Press, New York (1982) p157.
10. E. Fitzer, W. Hüttner and L. M. Manocha, *Carbon* **18** (1980) p291.
11. J. L. White and P. M. Sheaffer, *Carbon* **27** (1989) p697.
12. S. Kimura, E. Yasuda, K. Yasuda, Y. Tanabe, K. Kawamura and M. Inagaki, *Tanso* **125** (1986) p62.
13. Y. Hishiyama, M. Inagaki, S. Kimura and S. Yamada, *Carbon* **12** (1974) p249.
14. J. E. Zimmer and J. L. White, *Carbon* **21** (1983) p323.
15. J. H. Cranmer, I. G. Plotzker, L. H. Peebles Jr. and D. R. Uhlmann, *Carbon* **21** (1983) p201.
16. J. E. Zimmer and R. L. Weitz, *Carbon* **26** (1988) p579.
17. J. Dubois, C. Agache and J. L. White, *Metallography* **3** (1970) p337.
18. J. Jortner, *Carbon* **24** (1986) p603.
19. L. Boyne, D. Cook, J. Hill and K. Turner, Proc. 4th London Int. Carbon and Graphite Conf., Soc. of Chemical Industry, London (1974) p215.
20. B. L. Butler, D. A. Northrup and T. R. Guess, *J. Adhesion* **5** (1973) p161.
21. Y. Tanabe and E. Yasuda, Report of the Research Laboratory of Engineering Materials, Tokyo Institute of Technology **17** (1992) p137.

ACKNOWLEDGEMENTS

S. P. Appleyard would like to acknowledge the financial support of the Science and Engineering Research Council (SERC), Swindon, Wiltshire, UK. and ICI Advanced Materials, ICI Wilton Research Centre, Middlesbrough, Cleveland, UK.

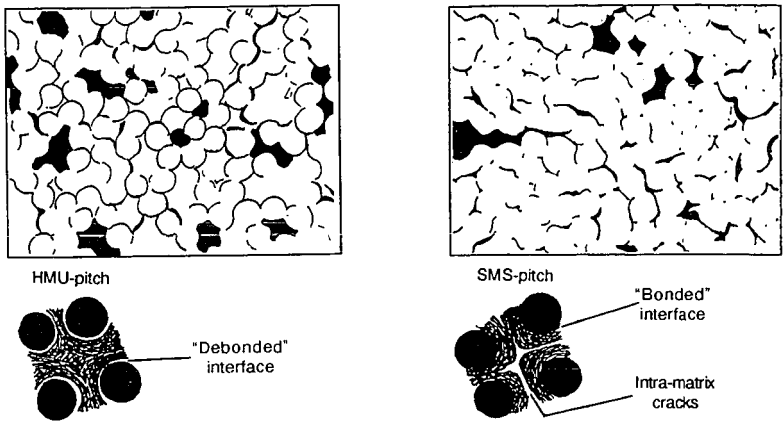


Figure 1
 Schematic illustrations of the different void network structures arising from the different fibre-matrix interactions that occurred in HMU-pitch and SMS-pitch composites on carbonisation.

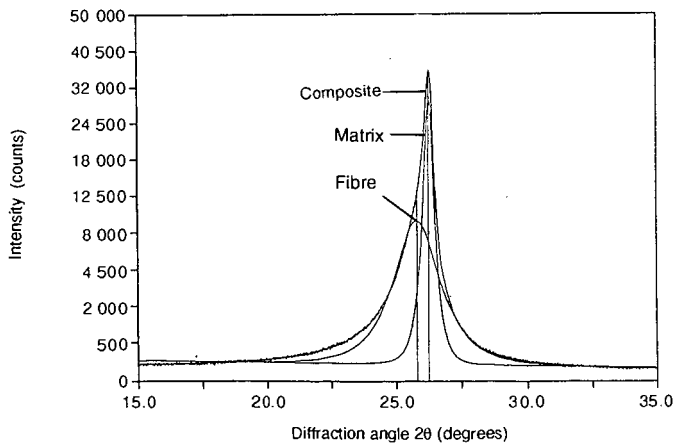


Figure 2
 X-ray diffraction profile given by HMU-pitch composite (carbonised, re-impregnated with pitch and then graphitised) with component fibre and matrix profiles obtained by computational deconvolution of the intensity profile.

EVALUATION OF RESIDUAL SHALE OILS AS FEEDSTOCKS FOR VALUABLE CARBON MATERIALS

You Qing Fei and Frank Derbyshire
Center for Applied Energy Research, University of Kentucky,
3572 Iron Works Pike, Lexington, KY 40511-8433

Keywords: Shale oil, carbonization, solvent extraction

INTRODUCTION

Oil shale represents one of the largest fossil fuel resources in the US and in other parts of the world. Beginning in the 1970s until recently, there was considerable research and development activity directed primarily to technologies for the production of transportation fuels from oil shale. Due to the low cost of petroleum, as with other alternate fuel strategies, oil shale processing is not economically viable at present. However, future scenarios can be envisaged in which non-petroleum resources may be expected to contribute to the demand for hydrocarbon fuels and chemicals, with the expectation that process technologies can be rendered economically attractive.

There is potential to improve the economics of oil shale utilization through broadening the spectrum of products that can be derived from this resource, and producing added-value materials that are either unavailable or more difficult to produce from other sources. This concept is by no means original. The history of oil shale development shows that most attempts to commercialize oil shale technology have relied upon the marketing of by-products [1]. These have included asphalts, construction bricks, cement, soil additives, town gas, lamp oil, rock wool insulation, ammonia, sulphur, paraffin, olefins and other chemicals, and power generation.

In this context, we have conducted investigations to assess the potential for producing premium carbon materials from shale oil residues. Retorted shale oils generally contain more high-boiling fractions than petroleum crudes [2,3]. This is especially true for eastern US shale oils. These properties make shale oils very attractive as carbon sources because the heavy fractions have high carbon contents. Another characteristic of shale oils is their high nitrogen content, which presents difficulties also in upgrading these liquids to clean fuels because extensive and deep hydrogenation is required. The nitrogen-containing species are more concentrated in the higher boiling fractions and accentuate the problem [4,5]. On the other hand, the nitrogen-containing compounds can become highly valuable feedstocks or chemicals if they are separated collectively or individually from shale oils.

We have already reported the successful production of isotropic carbon fibers and activated carbon fibers from the asphaltene fraction of residual shale oil produced from eastern US shale by the Kentort process [6, 7]. While the mechanical properties of the carbon fibers have yet to be assessed, the presence of nitrogen has been shown to enhance the catalytic properties of activated carbon fibers for reactions such as the ambient-temperature oxidation of SO₂ [8], and the nitrogen content is believed to contribute to the wide pore structure that is formed in the activated fibers [7,9].

As the maltene fraction of the shale oil residue has a much lower nitrogen content than the asphaltene fraction, it may be more suitable for the synthesis of other forms of carbon. In this paper, we present the results of studies to investigate the carbonization properties of this material, and to determine the potential for generating a pitch with high mesophase (a carbonaceous liquid crystal) content that could serve as a precursor for the production of materials such as needle cokes (a highly-oriented and graphitizable carbon) for the manufacture of graphite electrodes, and high-performance carbon fibers.

EXPERIMENTAL

A shale oil residue (SOR), produced in the Kentort II process from eastern oil shale [10,11], was used in the study. This residual oil was collected in an electrostatic precipitator and comprised 70-80 wt% of the total oil products from the retort. The sample was further fractionated by extraction with boiling hexane in a Soxhlet apparatus to obtain fractions with different heteroatom contents or polarity [12], namely, hexane-soluble (HS) and hexane-insoluble fractions. The parent shale oil sample and the extracted fractions were subjected to elemental and ¹H and ¹³C-NMR analyses.

Carbonization reactions were conducted both at atmospheric pressure and elevated pressure. Atmospheric pressure carbonization was performed in a Pyrex tube. Samples were heated in the tube reactor under nitrogen flow at 440 °C for 4h, in a vertical electric furnace. Pressurized

carbonization was conducted using a stainless steel tubing bomb ($\phi 1'' \times 4''$) [13, 14]. The bomb was charged with 15-20g of sample and placed in a sand bath preheated at 440-500 °C for a reaction time of 4- 6 h. The reaction pressure was maintained at 700 kPa by pressurizing the bomb with nitrogen before the carbonization reaction and automatically releasing excess pressure through a relief nozzle over the course of the experiment. The carbonized products were weighed and further characterized by elemental analysis and optical microscopy (Leitz, MVP2), using polarized light, after mounting and polishing.

RESULTS AND DISCUSSIONS

Almost the same yields of hexane-soluble (SOR-HS) and hexane-insoluble (SOR-HI) fractions were obtained upon extraction. This means that the eastern crude shale oil contains 30-40 wt% of asphaltenes, in comparison with western shale oils which have less than 5 wt% [2,3]. Table 1 shows some analytical data for the parent shale oil and the extracted fractions. In the order of SOR-HS, parent SOR and SOR-HI, the aromaticity increased and the H/C atomic ratio decreased. Aliphatic components are concentrated in the maltene (SOR-HS) fraction which has correspondingly low aromaticity. Sulfur is distributed evenly in both extracted fractions although it is to be noted that the sulfur concentration is much higher than found in other shale oils [2,3]. About 85% of the total nitrogen in the parent shale oil is concentrated in the SOR-HI fraction, where nitrogen content is about six times higher than that of SOR-HS.

Figure 1 shows the optical texture of products obtained by atmospheric pressure carbonization of the parent shale oil and the hexane soluble fraction. Both feeds produced mosaic texture cokes. The product from the parent shale oil has a fine mosaic texture (about 5 μm in size), while larger isochromatic units ($\sim 20 \mu\text{m}$ size) were observed in the SOR-HS coke. The hexane insoluble fraction (SOR-HI) also gave a fine mosaic texture very similar to that of the parent shale oil, possibly because the presence of the HI fraction dominates the carbonization progress, as indicated by carbonization yield in Table 2. The hexane soluble fraction alone gave a yield of only 8 wt %, whereas it was 46 wt% for the hexane-insoluble fraction. The yield for the parent shale oil was 26 wt%, essentially following the additive rule.

The optical micrographs of products obtained by pressurized carbonization of the shale oil and the hexane-soluble fraction are shown in Figure 2. Under these conditions, excellent flow domain textures were formed from the SOR-HS fraction. The full-range shale oil gave a mosaic texture, $\sim 20 \mu\text{m}$, larger than that obtained under atmospheric pressure. The effects of using elevated carbonization pressure have been reported to be favorable for anisotropy development for many other heavy oils, and it has been employed commercially to produce needle cokes [14]. It has been reported that a western shale oil and its maltene fraction also produce mosaic texture cokes upon the atmospheric carbonization, even after various preheat treatments [15, 16]. These results are consistent with the experiment results described above, although there may be differences in composition, structure and reactivity between the eastern and western shale oils. The experiment results indicates the importance of both solvent fractionation and overpressure to the carbonization of shale oil products. The results of the present study further suggest that the maltene fraction of eastern shale oil may be used to produce mesophase pitches for the synthesis of high-performance carbon fibers, or for premium coke production if sulfur and nitrogen contents are acceptable. Elemental analyses of green cokes shows that much lower nitrogen cokes are produced by using the maltene fractions rather than the full-range shale oil, Table 3.

The influence of carbonization conditions on coke yield can also be seen in Table 2. Pressurized carbonization can substantially increase the yield. Notably, the yield from the maltene fraction was increased by a factor of about four at 700 kPa. The effects of high pressure and a closed system will be to prevent the escape of volatile components and cracked products and retain a higher proportion of the precursor in the liquid phase. The coke yield also reflects the high reactivity of the SOR-HI fraction: there was only a 20% increase in yield upon going to pressurized carbonization.

Based upon previous findings [6,7] and the results of the present investigation, at least one scheme can be proposed for the more effective use of residual shale oils, Figure 3. The first step involves solvent separation into maltene and asphaltene fractions. Deasphalting processes have been used to prepare feedstocks for delayed coking in order to produce high grade cokes from petroleum heavy oils and lower the impurity contents (basically metals, such Ni and V) of the coke products. The same step seems necessary to render shale oils suitable for premium coke production, although the reasons appear to be somewhat different.

The asphaltene fraction from shale oil contains a high concentration of nitrogen species and has a high coking reactivity that can inhibit mesophase development [5]. The nitrogen-containing species also tend to be retained in the resultant cokes, and could cause puffing problems at graphitization. Although the sulfurs in the SOR-HS may also result in puffing, desulphurization can be achieved relatively easily by mild hydrogenation [17]. Thus, by removing asphaltenes, a material can be obtained that would be a suitable precursor for the production of needle cokes, or a mesophase pitch for the manufacture of high performance carbon fibers. Alternatively, maltene fractions may be completely refined to produce liquid fuels by conventional catalytic upgrading, since most of problematic nitrogen-containing species are removed.

The asphaltene fractions can be used as a source of specialty carbons with high nitrogen content. The combustion of such high nitrogen-content fuels could result in unacceptable emission of nitrogen oxides [18]. The production of isotropic carbon fibers and activated carbon fibers with unique properties may be an example of their practical utilization. Thus, starting with a heavy shale oil, we may produce a variety of valuable carbon materials in the form of pitch, coke and carbon fibers, with optical texture ranging from isotropic, fine mosaic to flow domain.

REFERENCES

1. C.F. Knutson, B.F. Russel and G.F. Dana, Proc. 20th Oil Shale Symposium, Colorado School of Mine, Golden, CO, USA, 1987, p217.
2. C.S. Scouten, In Fuel Science and Technology Handbook, edited by James G. Speight, published by Marcel Dekker, Inc. New York and Basel, (1990), p1008.
3. Pery Nowacki, In Oil Shale Technical Data Handbook, Published by Noyes Data Co., 1981, p19.
4. J.W. Bunger, P.A.V. Devineni and D.E. Cogswell, Reprint, American Chemical Society, Div. Fuel Chemistry, 37(2), 581(1992).
5. Pinky Udaja, Gregory J. Duffy and Martin D. Chensee, "Coking reactivities of Australian shale oils", Fuel, 69(9), 1150(1990).
6. Y.Q. Fei, F. Derbyshire and T. Robl, "Carbon fibers and activated carbon fibers from shale oil residue", Preprints, Am. Chem. Soc., Div. Fuel Chemistry, 38(2) 427(1993).
7. Y.Q. Fei, F. Derbyshire, M. Jagtoyen and I. Mochida, "Advantages of producing carbon fibers and activated carbon fibers from shale oils", Proc., Eastern Oil Shale Symposium, Lexington, KY, USA, Nov.16-19, 1993, p38.
8. F. Derbyshire, Y.Q. Fei, M. Jagtoyen and I. Mochida, Abstracts, International Workshop: Novel Technology for DeSOx and NOx, Fukuoka, Japan, Jan., 1994.
9. Y.Q. Fei, M. Jagtoyen, F. Derbyshire and I. Mochida, "Activated carbon fibers from petroleum, shale oil and coal liquids", Ext. Abstracts and Program, International Conference on Carbon, Granada, Spain, June 3-8, p.666, 1994.
10. S.D. Carter, T. Robl, A.M. Rubel and D.N. Taulbee, "Processing of Eastern US Oil Shale in a Mutistaged Fluidized Bed System", Fuel, 69(9), 1124(1990):
11. S.D. Carter, A.M. Rubel, T. Robl and D.N. Taulbee, "The development of the Kentort II process for Eastern Oil Shale", Final Report to DoE, Contract No. DE-FC21-86LC11086, May 1990.
12. Y.Q. Fei, K. Sakanishi, Y.N. Sun, R. Yamashita and I. Mochida, Fuel, 69(2), 261 (1990).
13. I. Mochida, Y.Q. Fei and Y. Korai, "A study of the carbonization of ethylene tar pitch and needle coke formation", Fuel, 69(6), 667(1990)
14. I. Mochida, K. Fujimoto and T. Oyama, In Chemistry and Physics of Carbon, Vol.24, edited by P. Thrower, published by Marcel Dekker, Inc., 1994, p111
15. M.A. Sadeghi, V.L. Weinberg and T.F. Yen, "Alternative precursors for mesophase formation", Extended Abstracts and Program, American Conf. Carbon, 1983, p116.
16. M.A. Sadeghi, V.L. Weinberg and T.F. Yen, "Shale oil delayed coking products utilization for manufacturing graphites" Preprints, Am. Chem. Soc., Div. Fuel Chemistry, 29(3), 224(1984)
17. See Ref. 2, p199.
18. R.K. Lyon and J.E. Hardy, "Combustion of spent shale and other nitrogenous chars", Combustion and Flame, 51,105(1983).

Table 1 Analytical data for the parent shale oil and fractions

Sample ID	Yield (wt%)	Elemental Analysis(wt%)				Atomic Ratio		fa
		C	H	N	S	H/C	N/C(x100)	
SOR	–	82.02	8.58	1.38	1.84	1.26	1.47	0.57
SOR-HS	52	82.55	10.21	0.41	1.85	1.48	0.43	0.45
SOR-HI	48	81.39	6.88	2.49	1.81	1.01	2.62	0.71

* SOR, parent shale oil; HS, hexane-soluble fraction; HI, hexane-insoluble fraction; fa, fraction of aromatic carbon

Table 2 Carbonization yield (wt%) of parent shale oil and fractions

Feedstock	Atmospheric pressure	Pressurized (700 kPa)
SOR	26	40
SOR-HS	8	31
SOR-HI	46	57

* SOR, parent shale oil; HS, hexane-soluble fraction; HI, hexane-insoluble fraction

Table 3 Properties of green cokes obtained from parent residual shale oil and HS fraction

Feedstock	SOR	SOR-HS
Carbonization condition	440 °C-700 kPa	440 °C-700 kPa
Optical texture	Mosaic	Flow
N content (wt%)	3.22	1.08

* SOR, parent shale oil; HS, hexane-soluble fraction.

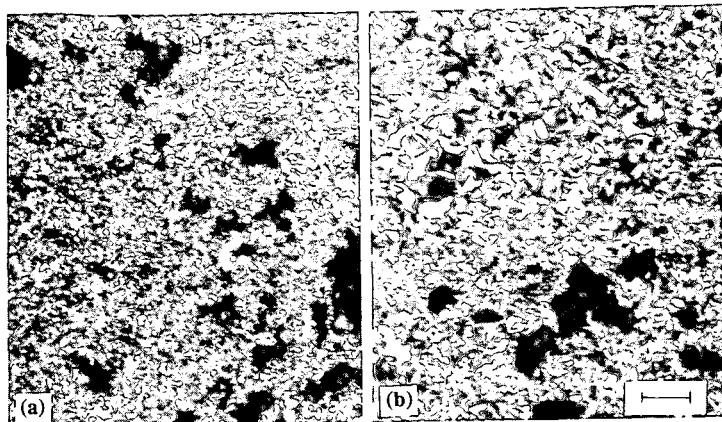


Figure 1 Optical texture of products carbonized at atmospheric pressure from: (a) Parent SOR, (b) Hexane-soluble fraction of SOR

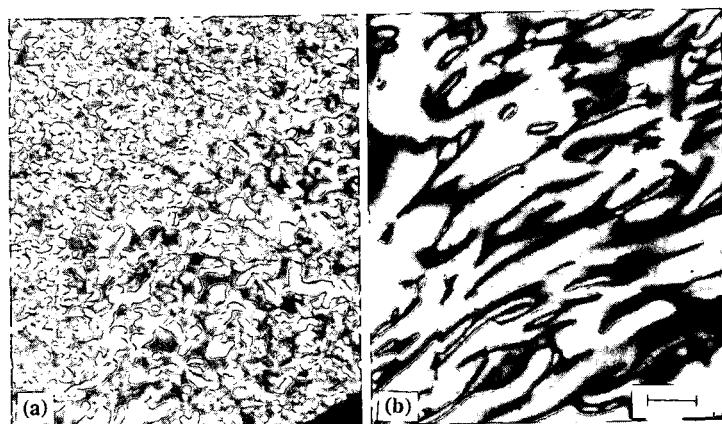


Figure 2 Optical texture of products carbonized under pressure (700 kPa) from: (a) Parent SOR, (b) Hexane-soluble fraction of SOR

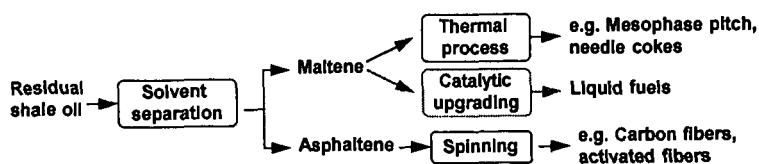


Figure 3 Illustration of a value-adding route for utilization of residual shale oils and resultant intermediate and final products

**PRODUCING VAPOR GROWN CARBON FIBERS WITH
HIGH SULFUR COAL WITHOUT SO₂ EMISSIONS**

R. Alig, M. Lake, J. Guth, and D. Burton
Applied Sciences, Inc.
P.O. Box 579
Cedarville, OH 45314

Keywords: SO₂ Control Technologies, Coal Pyrolysis, Organic Sulfur Removal

ABSTRACT

This paper describes the development of a unique process that produces a highly graphitic, vapor grown carbon fiber (VGCF) from the gas phase in pound quantities. Past vapor grown carbon fiber progress has stagnated because the iron catalyst did not grow filaments profusely enough to make a practical continuous reactor. It has been found that adding H₂S at an equimolar level with the iron catalyst, the filament formation vastly increases. Coal is desirable as a sulfur source, for it eliminates the need for handling toxic H₂S, and it is a very low cost hydrocarbon supply for the process. We show that Ohio, high-sulfur coal containing 2.5 to 4.6% sulfur accomplishes both tasks. There is also evidence that sulfur from the coal remains with the carbon fiber catalyst during the reaction and does not exhaust as SO₂ into the atmosphere.

INTRODUCTION

Carbon fibers have been of practical interest within the industrial community for over a century; Thomas Edison tried them as filaments for light bulbs. The Air Force started carbon fiber development for aerospace in the 1950's because of their mechanical and electrical shielding properties. These fibers were found to be stronger than steel, stiffer than titanium, and yet lighter than aluminum. Today, golf clubs, fishing poles, and tennis rackets are typical uses in the commercial sector.

A. Commercial fibers

Commercial carbon fiber uses are limited because they are more expensive than competing metals for engineering applications. Furthermore, their diameter is 8 μ , which is larger than normal fillers, such as carbon black, for reinforcement. This imposes expensive and limited processing techniques into composite applications. Hand lay-ups and slow pultrusion techniques are the norm; straight injection molding is out of the question. The total U.S. market for carbon fibers in 1990 was 6 million lb, of which 0.8 million lb were for the recreational market at an average cost of 23 \$/lb for the carbon fiber¹. For comparison: 3 billion lb of carbon black were shipped to rubber manufacturers in 1992² at an average cost of 0.25 \$/lb.

Commercial carbon fibers are formed from polymer precursors such as polyacrylonitrile (PAN) or petroleum pitch. The precursor is extruded or spun similar to textiles into a continuous filament or thread, oxidized under tension to 200^o C, and followed by slow heating in the absence of air to 1000^o C to carbonize the fiber. Sometimes, the carbon fiber is given additional heating up to 3000^o C to develop higher degrees of graphitization, which is needed for expensive ultra-high strength (2000 \$/lb range) applications.

B. Vapor grown carbon fiber

This paper is based upon a unique form of carbon fiber requiring no precursor filament. It is called vapor grown carbon fiber (VGCF), known as PYROGRAF IIITM. From initial inventions at General Motors, the patents were licensed to Applied Sciences, Inc. in 1992 for further development and manufacture. The process began by early workers, exposing vapor phase metals, generally iron, supported on inert substrates while exposed to hydrocarbons and hydrogen³ at a temperature in the 1000 - 1150^o C. range. This catalyzed the growth of long, slender, partially graphitic filaments⁴ as

shown in Figure 1. Although these methods remained essentially batch processes and too inefficient for mass production, this VGCF when subsequently heat-treated has a thermal conductivity of 1950 W/m-K (highest value found in nature except for diamond) and is sold as a carbon/carbon composite for aerospace thermal management materials. This was followed by attempts at a continuous process by injecting and dispersing the iron catalyst particles directly into the gas stream, and eliminating the use of a substrate for growth^{6,7}. This was still non-productive; the iron catalyst did not grow filaments profusely enough to make a practical continuous reactor. A breakthrough occurred when it was found and confirmed from early work in the 1950's by Kauffman and Griffiths⁸ that sulfur was vital to fiber formation. Adding hydrogen sulfide (H₂S) at an equimolar level with the iron catalyst, vastly increase^{9,10} the filament formation making a continuous reactor practical (Figure 2). We believe that the sulfur is incorporated in the fiber by being adsorbed onto the catalyst, and subsequently overcoated with graphite.

Figure 3 shows scanning electron micrographs of vapor grown carbon fibers grown by a gas phase process in comparison with typical continuous commercial carbon fibers. The diameter of PYROGRAF III generally averages 0.2 μ as produced, while commercial fibers are 8 μ in diameter. Due to the nature of the gas phase generation, the fibers become entangled during growth and are not continuous like commercial fibers. The length/diameter ratio for PYROGRAF III ranges from 40 to 200. Due to the process and purity with which carbon is formed into the fiber, VGCF is highly graphitized (Table 2) and the stress/strain properties for 7.5 μ VGCF (Figure 4) results in similar or higher property ranges than commercial carbon fibers. The smaller diameter and entanglements of the PYROGRAF III defy measurement.

C. Coal

Most of the VGCF made to date used laboratory grade methane, benzene, acetylene, etc. as a hydrocarbon source as a step toward reproducible results. Since we have developed one product line that can produce almost a pound per hour, natural gas is frequently used for high volume trials. Although the addition of H₂S was instrumental in achieving this improvement, it is used with great reluctance. Hydrogen sulfide is expensive, highly corrosive to rubber seals and metal fittings, flammable, and its toxicity is on a par with hydrogen cyanide.

This suggests that a fossil fuel such as Ohio high sulfur coal may be especially apropos for this problem since Ohio coal production has gone from 55 million tons in 1970 to 33 million tons in 1990. Ohio coal's high sulfur content is most responsible for this decline, which is projected to go lower due to the 1990 Clean Air Act Amendment. Furthermore, coal would have a tremendous effect on the eventual price of the fiber. The hydrocarbon is the most expensive cost item, followed by the electric oven energy and the catalyst. Although the energy consumption and output capabilities are not yet optimized for a total cost picture, the formulations that will be discussed later show that coal at 30 \$/ton not only drastically reduces the cost of the carbon source, but totally eliminates the price of the sulfur:

PYROGRAF III MATERIAL COST COMPARISON

	Control Methane Only (\$/lb)	Control Natural gas only (\$/lb)	Trial 1 94% N.G. 6% Coal (\$/lb)	Trial 2 100% Coal (\$/lb)
Sulfur Source	0.189	0.194	0	0
Carbon Source	69.83	0.44	0.419	0.067

EXPERIMENTAL

In this experiment, a reactor that normally uses a feedstock mixture of 99.9% pure methane was converted to enable use of coal as the hydrocarbon feedstock (Figure 3). Helium is bubbled through liquid iron pentacarbonyl to provide Fe catalyst particles, and 99.3% pure H₂S gas is simultaneously injected into the 1100° C reactor. A typical control formulation that produces a 25% yield is shown in Table I. A screw type apparatus was assembled to feed the coal and driven by a variable speed motor. It is similar to commercial equipment except the feed box is sealed from the air; otherwise, it may cause combustion as the coal enters the reactor. A carrier gas is used to transport the coal dust from the screw feed into the reactor hot zone.

Two trials using coal are shown in Table 1. In Trial 1, the hypothesis is that sulfur-bearing coal can replace H₂S as the source of sulfur in the reaction. Coal and methane were used as the hydrocarbon feedstock. The formulation was developed so that the sulfur content in the coal was equivalent (1.6 H₂S/Fe(CO), molar ratio) to the sulfur in the "control" formulation using methane and hydrogen sulfide. Ohio #8 Coal from CONSOL Inc., at 4.71% total sulfur and 46.6% total carbon, was pulverized to less than 63 μ . Methane was the carrier gas at a rate calculated to maintain a similar 1.6 molar sulfur/carbon ratio as the "control". It was assumed that all the sulfur in the coal was converted to hydrogen sulfide.

Trial 2 was to test the hypothesis that coal could serve as the only supply of the hydrocarbon and sulfur, and produce vapor grown carbon fiber. The pulverized coal was carried into the reactor with a non-hydrocarbon carrier (hydrogen). Upper Freeport Seam coal was obtained from Kaiser Engrs. with 2.5 % total sulfur and an estimated 65% carbon content. In this case without methane dilution, the molar sulfur/catalyst ratio is 4.5, which is considerably higher than the minimum 1/1 ratio for good filament formation.

RESULTS AND DISCUSSION

Carbon yield is here defined as the fraction of fiber harvested to the total carbon introduced into the reaction from all hydrocarbon sources. In the "control", vapor grown carbon is routinely produced with a yield of 25% with a 2% standard deviation. In Trial 1, with coal, methane, and no H₂S, the carbon yield is 19%. The photomicrograph in Figure 6 shows very good growth and confirms that the sulfur contained in the coal plays an active role in the catalytic process, and can potentially replace the need for using H₂S in the reaction.

The sulfur content in coal is well beyond the optimum amount for the formation of carbon fibers. Figure 6, reproduced from one of our prior papers¹⁰, shows SEM photomicrographs of carbon fiber produced with H₂S/Fe(CO), ratios of 0, 1.4/1 and 17/1. The sparse fiber in the photo without sulfur clearly illustrates the need for sulfur. However, the photo at the very high 17/1 ratio still produces very good carbon fiber; the fiber length is shorter, and tends to be more jagged and the soot content increases. Nevertheless, this leads to the possibility that high sulfur coal in spite of its problems for other uses may be a unique asset for the production of acceptable vapor grown carbon fiber.

In Trial 2, coal is the only source of both hydrocarbon and sulfur; a yield of 47% was obtained and a SEM photomicrograph is shown in Figure 5. There is good, but shorter fiber formation with a fair amount of soot and perhaps some ash. From past experience, the high carbon yield is anticipated, for we know that at extremely high sulfur levels, only soot will be formed. Nevertheless, these results support the conclusion that the inherent carbon in coal is actively pyrolyzed to products which participate in the catalytic fiber nucleation and growth process.

Photomicrographs are the basic estimate of fiber formation. However, X-ray diffraction can estimate the graphitic ordering and is the crucial property for assuring the quality of the fiber's strength and conductivity. Samples from the trials were analyzed by X-ray diffraction; Table 2 shows that the fiber samples from coal Trials 1 and 2 have a graphitization index that is typical for low modulus commercial fiber.

In earlier trials that rely on introducing H₂S into a pure methane feedstock at equivalent ratios with the catalyst, periodic analysis has been made of the exhaust. To date, sulfur has not been detected in the exhaust. This could be explained by the proposal¹⁰ that the sulfur dissolves in such large amounts that it melts the iron catalyst and thus stays with the catalyst at the base of the fiber. How much sulfur can be dissolved as the sulfur increases is unknown; there is a limit where fiber is no longer formed. A packed column gas chromatograph (GC) with thermal conductivity detector was used to estimate the composition of the exhaust gases of a series of coal trials when the sulfur was running at 4.5 times the usual amount (Trial 2) and the presence of sulfur was not detected. This instrument does not have the sensitivity to measure nitrogen or sulfur compounds below about 0.1-1 percent. Gastec detection tubes capable of detecting sulfur dioxide concentrations of 0.25 ppm and above were also used and no SO₂ was detected. Future work is needed with a capillary column GC with dedicated nitrogen and sulfur detectors.

Nevertheless, the data does support the theory that the sulfur does unite with the catalyst during fiber formation and would eliminate or reduce the release of harmful sulfur compounds into the atmosphere. Future work should also address the sulfur content, if any, in the residual ash over a wide range of sulfur/catalyst ratios. Although further work is needed to assess the effects of the organic and ash content variation in coal, their presence does not prevent the growth of a carbon fiber with graphitic ordering. For some applications such as rubber reinforcement, it is possible that the sulfur content in the fiber may be uniquely desirable and enhance the bonding during the rubber vulcanization process.

While these studies indicate the viability of using high sulfur coal as the hydrocarbon feedstock in production of VGCF, in practice, the high percentage of sulfur in various coals, as well as the variability of the percentage of sulfur in coal, will most likely mandate a combination of hydrocarbon feedstocks in order to maintain the process balance needed for optimum production. The role of coal in contributing to the hydrocarbon balance, as well as the sulfur balance, has significant implications.

CONCLUSIONS

It has been demonstrated that high sulfur coal can be used to make VGCF, contributing both carbon and sulfur to the reaction. This work suggests an ecologically safe process for utilization of high sulfur coal. If future trials continue to confirm these conclusions, the economic impact of coal on the price of carbon fiber will open new applications for carbon fiber in rubber reinforcements, cement, composites for automobiles, electronics, and aerospace components.

ACKNOWLEDGEMENT

This research was supported in part by the Ohio Coal Development Office/Ohio Department of Development under Grant Number CDO/R-922-8. The authors also gratefully acknowledge the contribution of Dr. Gary Tibbetts, General Motors NAO Research & Development, for his assistance and pioneering work that has made vapor grown carbon fibers a commercial reality, Dr. David Anderson from the University of Dayton Research Institute in providing X-ray analysis, and much assistance from the OCDO staff in performance of this work.

REFERENCES

1. C. Petersen, **ADVANCED COMPOSITES**, March/April 1994, pp 20.
2. **CARBON LINES** Vol. 4, No. 1, March 1993, Newsletter by Huber engineered Carbons Division.
3. G.G. Tibbetts, **Carbon** 30, 399 (1992).
4. J.L. Kaee, **Carbon** 23, 665 (1985).
5. M. Endo and T. Koyama, Japanese patent 1983-180615, Oct 22 (1983).
6. Y. Komatsu and J. Endo, Japanese patent 60-32818, Feb 22 (1985).
7. K. Arakawa, U.S. Patent 4,572,813, Feb. 25 (1986).
8. H.F. Kauffman and D.J. Griffiths, U. S. patent 2,796,331, June 18 (1957).
9. G.G. Tibbetts, D.W. Gorkiewicz, and R.L. Alig, **CARBON** 31, 809 (1993).
10. G. G. Tibbetts, C. A. Bernardo, D. W. Gorkiewicz, and R. L. Alig, "Effect of Sulfur on the Production of Carbon Fibers in the Vapor Phase" **CARBON**, 32, no. 4, pp. 569-576, (1994).

TABLE 1. TRIAL FORMULATIONS*

	CONTROL	TRIAL 1	TRIAL 2
METHANE	96.90	87.58	NONE
COAL	NONE	9.33	80.68
SULFUR	0.47	0.44	2.02
HYDROGEN	NONE	NONE	13.30
HELIUM	0.96	0.96	1.45
Fe(CO) ₅	1.68	1.69	2.55

* Formulations are in per cent by weight

TABLE 2. X-RAY DIFFRACTION ANALYSIS

HEAT TREAT (°C)	FIBER TYPE	D-Spacing (nm)	g _D * (%)
AS-GROWN	VGCF	.34490	--
1300	ex-PAN	.354	--
AS-GROWN	COAL & METHANE	.3459	--
AS-GROWN	COAL ONLY	.3451	--
2500	ex-PAN	.342	23
2500	VGCF	.3377	73
as-grown	PYROGRAF III	.3385	64
--	P-120	.3378	72

*g_D = (0.3340 - D-Spacing)/(0.3440 - 0.3354)

Fiber Nucleation and Growth Model

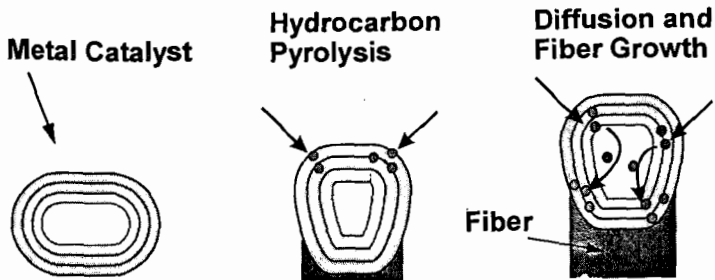


Figure 1. Fiber Nucleation and Growth Model

Carbon Fiber Process

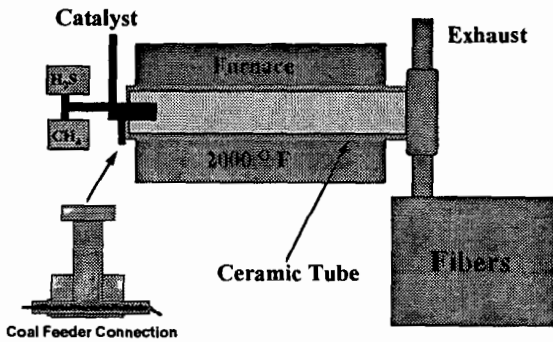


Figure 2. Carbon Fiber Processing

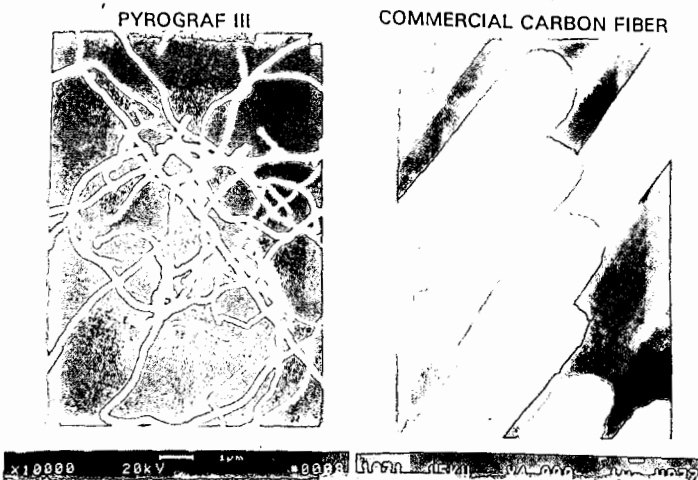


Figure 3. Scanning Electron Micrographs Comparing Vapor Grown Carbon Fiber with Commercial Carbon Fiber

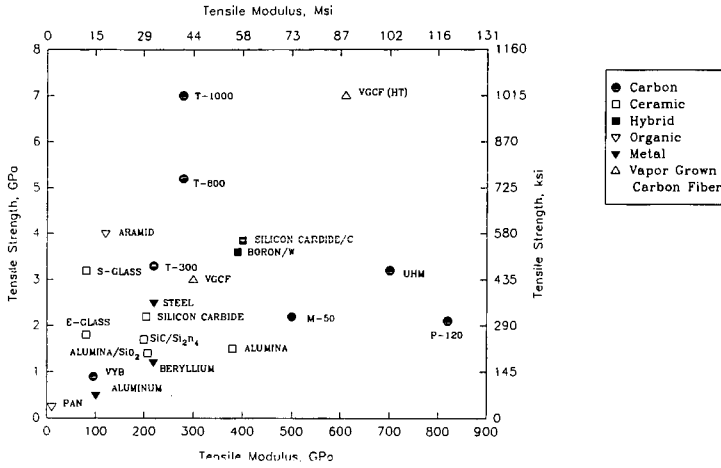


Figure 4. Tensile-Modulus Properties

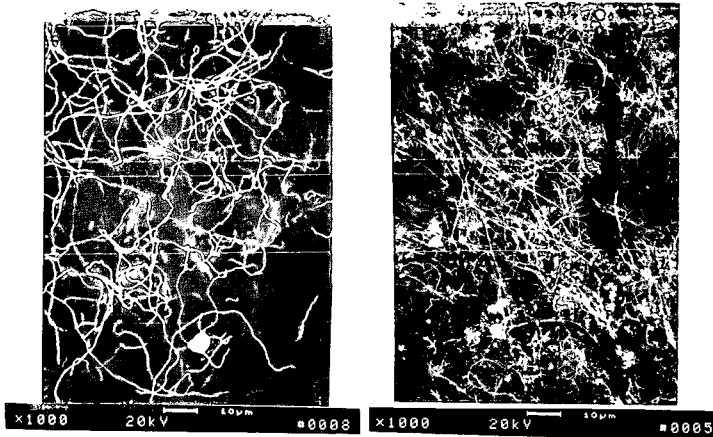


Figure 5. Coal Derived Fiber

Effect of H₂S on Fiber Growth

SEM Photomicrographs

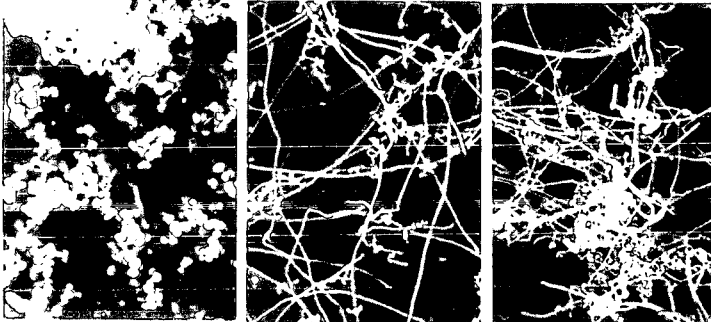


Figure 6.

No H₂S Flow

H₂S/Fe.(CO)₅=1.4/1

H₂S/Fe (CO)₅=17/1

THE PREPARATION OF FINE CARBIDE POWDERS FROM COAL SOLUTIONS

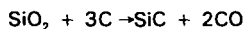
David. L. Morgan, Vladimir Cukan and Sara N. Prins
Division of Materials Science and Technology, CSIR
P O Box 395, 0001 Pretoria, South Africa.

Keywords: silicon carbide, coal solution, sol-gel.

INTRODUCTION

Non-oxide ceramics, such as silicon carbide [1], find use in applications requiring extreme hardness, chemical inertness and high-temperature strength. Transition metal carbides, such as tungsten carbides cemented with cobalt or nickel, are used extensively as wear components. Articles are generally fabricated by sintering pressed powder bodies at high temperatures. To maximise strength and hardness of the ceramic bodies, fine powders below 1 micron in size are needed together with small additions of sintering aids. Boron carbide plus carbon are used as sintering aids for silicon carbide. Very uniform dispersion of the sinter aid or binder metal with the carbide powder is necessary. This is achieved by milling the components together, often for many hours. The carbides are generally prepared by reacting the metal or oxide together with carbon. The low reactivity of particulate carbon means that high temperatures have to be used with extensive milling being required to reduce the particles to a suitable size. The end result of these requirements is that sinterable powders are expensive.

Fine oxide ceramic powders with very uniformly dispersed additives are prepared by the sol-gel process where the components are mixed as solutions or sols and the mixture then gelled [2]. The solvent is removed and the ceramic converted at relatively low temperature to fine, easily-sinterable powder. It would be very desirable to be able to extend those ideas to the preparation of fine carbide powders by bringing a carbon source into very intimate contact with an oxide followed by carbothermal reaction to the carbide e.g.:



However no low-cost carbon source has been readily available. Carbohydrates have been used in solution with colloidal silica sols but non-uniform drying could be expected [3]. Polycarbosilanes and silanes may be converted to silicon carbide but are very expensive [4]. Most organic polymers pyrolyse to carbon, but generally in low yield.

Coal solutions may be used as an effective and inexpensive source of carbon for the sol-gel preparation of silicon carbide. The coal molecules may also be brought into very intimate contact with the oxide by co-precipitating coal from solution together with an oxide gel under conditions of high shear. This approach is more general as maintaining both coal and metal oxide sol in solution together prior to gelling is not a simple matter. Absorbing coal molecules into a high surface area oxide is also effective. The coal is immobilised by gelling prior to solvent recovery.

We have prepared silicon carbide from coal solution by each of these three approaches [5]. The products from the co-gel and co-precipitation routes were both fine powders, with a very small content of fibrous whiskers whilst that prepared by the mixing route was predominantly fibrous in nature.

X-ray diffraction measurements showed that in all cases the silicon carbide was in the β -form, as would be expected from the low conversion temperature.

COAL SOLUTION

The coal solution was prepared by alkali-induced solubilisation of a medium-volatile bituminous coal in dimethylformamide (DMF) [6,7]. Over 90% of the organic part of suitable coals dissolve in DMF on addition of 10% (based on coal) of sodium or potassium hydroxide. The conditions for extraction are mild-atmospheric pressure,

temperature of 90 °C but strict exclusion of oxygen. The mineral components are removed by centrifugation and filtration giving a purified solution of "refcoal". The refcoal solutions used for carbide preparation had typically a concentration of 8% coal-derived material.

Refcoal solution gels on addition of 5% water or sufficient acid to neutralise the alkali present, giving a soft gel strong enough for a cylinder 2cm x 6cm high to be self-supporting.

The refcoal after removal of solvent contained less than 0,2% ash and gave 75% yield of carbon on pyrolysis at 1000 °C.

EXPERIMENTAL

The coal used was a flotation concentrate, with essentially all particles being smaller than 0,85 mm. The analysis is given in the Table.

PREPARATION OF COAL SOLUTION

Coal (5,0 kg), DMF (50 kg) and sodium hydroxide pearls (0,5 kg) were stirred together under nitrogen at 90 °C for 5 hours. The minerals and undissolved coal were removed by settling followed by filtration through polypropylene filter cloth. The clarified solution contained 8,0% dissolved coal material. The viscosity was 2,9 cP at 30 °C.

PREPARATION OF SILICON CARBIDE BY SOL-GEL ROUTE

A silica sol was prepared by mixing ethyl silicate (40% SiO₂, 7,5 kg) in DMF (3,5 kg) with 1% HCl solution in water (1,33 kg). The mixture warmed and became homogeneous over 60 minutes.

The silica sol was cooled to below 5 °C and rapidly mixed (within 5 seconds) with coal solution (50 kg), also cooled to below 5 °C. The mixture thickened and then gelled. The gel was broken up and the solvent removed under reduced pressure at 95 °C to give a coarse powder which was pressed into briquettes (~ 8 g mass) under high pressure. The briquettes were pyrolysed at 900 °C for 3 hours and then converted to silicon carbide by heating to 1500 °C for 7 hours in a stream of argon (15 l/min). After cooling under argon the briquettes were crushed to smaller than 1 mm and excess carbon burned off at 700 °C for 5 hours in a muffle furnace. Measurement of free silica showed 99,5% conversion although this may represent some re-oxidation during carbon burnoff. Sodium salts arising from the alkali present in the coal solution were removed with a dilute acid wash and the product was dried.

The silicon carbide was a fine grey powder. Size analysis gave a median particle size of 1,5 micron. SEM examination showed that the particles were made up of agglomerates of sub-micron particles. Whisker-like particles were virtually absent - a few could be found on active searching.

PREPARATION OF SILICON CARBIDE BY CO-PRECIPITATION ROUTE

Sodium silicate solution (300 ml, containing 18,0 g SiO₂ and 5,45 g Na₂O), sulphuric acid (48 ml, containing 8,5 g H₂SO₄) and coal solution (300 ml) were pumped separately but simultaneously over 5 minutes using peristaltic pumps into a reactor (30 ml) fitted with a high-shear mixer. The overflow of gelatinous co-precipitate was collected and recirculated through the high-shear mixer for 30 minutes at 100 ml/min.

The co-precipitate was dried and sodium sulphate removed by washing with water. The precursor powder was briquetted under pressure and converted to silicon carbide by heating to 1450 °C for 6 hours under flowing argon. Conversion of silica was complete. Excess carbon was burned off at 700 °C for 5 hours.

The silicon carbide was a fine grey powder with a median particle size of 3,5-5 micron. SEM examination showed that the particles were made up of agglomerates of sub-micron particles. Few whiskers were seen but there were

more than were present in the co-gelled product.

PREPARATION OF SILICON CARBIDE BY MIXING ROUTE

The precipitated silica used was Crosfield Neosyl GP, containing 88% SiO₂ and with a typical BET surface area of 200 m²/g. Precipitated silica (20,5 g, containing 18 g SiO₂) was mixed with coal solution (300 ml). Water (15 ml) was added to gel the coal solution. The solvent was removed to give a precursor which was converted to silicon carbide as above. The conversion of silica was total.

The silicon carbide after excess carbon burnoff formed a felt of fibrous material. SEM examination showed that the great bulk of the product was fibrous with some interspersed amorphous material.

DISCUSSION

The fineness and freedom from fibrous material of the silicon carbide prepared by the three different approaches from coal solution is clearly affected by the degree of inter-dispersion of the refoal with the silica. The sol-gel route would be expected to give the highest inter-dispersion of carbon and silica as the components had been mixed together in solution prior to gelling. The mixed precursor might be expected to have the poorest inter-dispersion with the co-precipitated precursor in between. The properties of the silicon carbide prepared from co-precipitated precursor were very similar to that prepared from the co-gel material which suggests that the inter-dispersion was also similar. This augurs well for successfully extending the co-precipitation route to the preparation of other carbides, because control of this method is simpler than that of co-gelling coal solutions with oxide sols. Clearly the properties of the silicon carbide prepared by the co-gel route are better than those of co-precipitate material. However the cost of silica from sodium silicate is very much less than that from ethyl silicate so that our further efforts are being concentrated on optimising the co-precipitation route, and on the introduction of homogeneously dispersed sintering aids.

ACKNOWLEDGEMENTS

The authors wish to thank the CSIR and the South African Department of Mineral and Energy Affairs, through the National Energy Council, for funding this work. Patents arising from the Project are held by Enerkom (Pty Ltd).

Technical assistance by Alpheus Bokaba, Tom Hardenberg and Samuel Sibanda is gratefully acknowledged.

REFERENCES

1. Y. Somiya and S. Inomata (eds.): Silicon Carbide Ceramics vols 1 and 2. Elsevier Science Publishers Ltd., London (1991).
2. L.L. Hench and J.K. West Chem. Rev, 1990 **90** 33.
3. A. Jubbe, A. Larbot, C. Guizard, L. Lot, J. Charpin and P. Bergez, Mat. Res. Bull. 1990 **25** 601.
4. R.M. Laine and F. Babonneau Chem. Mater. 1993 **5** 260.
5. D.L. Morgan and V. Cukan S.A. Patent No. 93/5725.
6. D.L. Morgan Preprints ACS Div. Fuel. Chem. 1992 **37(4)** 1996.
7. D.L. Morgan US Patent No. 5 120 430.

TABLE: COAL ANALYSIS

Moisture	0,7%
Ash	10,8
Vol. Mat.	22,6
Fixed carbon	65,9
DAF carbon	90,5
hydrogen	5,4
nitrogen	1,9

ACTIVATED CARBONS FROM NORTH DAKOTA LIGNITE AND LEONARDITE

Brian C. Young, Edwin S. Olson, Curtis L. Knudson, and Ronald C. Timpe
University of North Dakota Energy & Environmental Research Center (EERC)
Grand Forks, ND 58202

KEYWORDS: Leonardite activated carbons

INTRODUCTION

The EERC is undertaking a research and development program on carbon development, part of which is directed towards investigating the key parameters in the preparation of activated carbons from low-rank coals indigenous to North Dakota. Carbons have been prepared and characterized for potential sorption applications in flue gas and waste liquid streams.

Lignite, owing to its wide occurrence and variability in properties, has received significant attention as a precursor of active carbon manufacture. Mineral matter content and its alkaline nature are two highly variable properties that can have important consequences on the production of suitable activated carbons. Other factors affecting the production include carbonizing conditions, the activation agents, activation temperature, and activation time (1, 2). However, as previously noted, the relationship between the above factors and the sorption activity is particularly complex (2). Part of the difficulty is that sorption activity encompasses at least three parameters, namely, surface area, pore distribution, and surface acidity/basicity. The presence of mineral matter in the coal can affect not only carbonization but also the activation and subsequent sorption and desorption processes.

Lignite-based activated carbons typically have a low micropore volume, some 17% of the pores being micropores versus 35%–50% macropores (3). The macropores contribute little to the surface area and hence have a small impact on the adsorption process. Samaras, Diamadopoulos, and Sakellariopoulos (4) have recently shown that the removal of mineral matter improves the micropore volume of activated carbons since the mineral matter catalyzes the pyrolysis and carbonization reactions, leading to an enlargement of the pores. Several inorganic species, such as Fe, K, Mg, Ca, and Na are likely gasification catalysts, but the mechanism is not well understood. Removal of mineral matter from lignites decreases the reactivity of the chars towards carbon dioxide and oxygen (5) and produces random changes in the surface area as a result of structural changes (6).

As well as surface area and surface heterogeneity, the presence and structure of particular oxygen surface groups are also important for the adsorption of specific gases or vapors (7, 8). Basic oxygen groups with a pyronic structure, for instance, favor the adsorption of sulfur dioxide (9). Furthermore, Davini (10) has recently demonstrated that carbons containing a significant mineral matter content, particularly if an appreciable amount of iron is present, and an enhanced content of acidic oxygen groups have reduced capacity for SO₂ sorption.

This paper reports recent results of an investigation of demineralization, carbonization temperature, activation temperature, and activation time for one lignite and one leonardite from North Dakota. The majority of the work has been carried out with leonardite. This work is developing further data and understanding on leonardite char adsorbents reported earlier in a patent by Knudson (11).

EXPERIMENTAL

The feedstocks included a Beulah-Zap lignite and a Georesources leonardite. The coals were crushed, ground, and sieved in the usual manner to recover the -10 x 30- or -12 x 30-mesh fraction for testing. The coal analyses (thermogravimetric [TGA] and proximate) are shown in Table 1. The composition of the mineral matter of the leonardite by x-ray fluorescence was also determined.

Two reactors were used to produce the chars, a large capacity (100 grams) TGA unit and a nominally 12-kg capacity Cress kiln (model X31TC). The latter has a bottom distributor plate through which gas, preheated by the kiln, enters to permeate the bed. The chars were activated in the TGA unit or a Lindbergh Type 59344 furnace (TF) incorporating a 19-inch-long by 1-inch-diameter Vycor tube.

A representative sample of the leonardite containing a high mineral matter content was physically and chemically cleaned. Physical cleaning involved float-sink with Certi-grav and using the 1.4 and 1.6 float fractions. Both hydrochloric and hydrofluoric acids were used for chemical cleaning.

The initial carbonization conditions were as follows:

1. TGA unit — Approximately 50 g of feed was carbonized at 700°C to 850°C under N₂ for up to 1 hour followed by steam activation at the same temperature for up to 1 hour.
2. Kiln vessel — Approximately 12 kg of feed was at 480°C under N₂ for 1 hour. Subsequently, the leonardite was carbonized at different temperatures (see below).

Table 2 lists the conditions for activating the leonardite carbonized at 480°C in the kiln. Once the optimum activation temperature was established, the optimum activation time was determined by repeating the test conditions. Table 3 shows the variables used in optimizing the conditions for sorbent preparation from the leonardite. Beulah lignite was activated at 750°C for 20 minutes under 20% steam in nitrogen.

TABLE 1
Coal and Char Proximate Analyses

Coal	Carbonization Temp., °C	Activation Temp., °C	wt%, ar* Moisture	wt%, mf** Volatiles	wt%, mf Fixed C	wt%, mf Ash
Geo*	NA**	NA	32.6	44.1	27.6	28.3
Geo-1.6 Float	NA	NA	22.3	38.4	51.7	9.9
Geo-1.4 Float	NA	NA	42.9	51.2	41.8	7.0
Beulah	NA	NA	31.8	43.9	49.9	6.2
Geo	480	NA	5.3	32.8	47.2	20.0
Geo	480	700	1.1	8.7	52.6	38.6
Geo	480	750	1.1	8.4	53.6	38.0
Geo	480	800	0.9	7.0	57.6	35.5
Beulah	750	750	1.6	6.6	79.7	13.7

* As-received.
 ** Moisture-free.
 * Georesources leonardite.
 ** Not applicable.

TABLE 2
Test Conditions for Activating Georesources Leonardite Char Carbonized at 480°C in the Kiln Reactor*

Test No.	Sample Size, g	Reactor	Temperature, °C
1	10	TGA	700
2	10	TGA	750
3	10	TGA	800
4	10	TGA	850
5	50	TF	800
6	50	TF	850
7	50	TF	900
8	50	TF	950
9	50	TF	1000

* All samples were activated in 20% steam in nitrogen for 10 minutes.

TABLE 3
Test Conditions for Optimizing Char Sorbent Preparation

Variable	Condition
Activation Time under Steam	0, 10, 20, 40, 60 minutes
Coal Cleaning Prior to Charring	1.4, 1.6 Float; HCl, HCl/HF leach
Carbonization Temp.	350, 480, 550°C
Carbonization Temp.	350, 480, 550°C
Activation Temp.	750°C
Activation Gas	Steam, steam/O ₂
Gas-Char Contact Time	10, 20, 20 (steam)/5 (O ₂) minutes

The activating agent was steam in nitrogen, with an approximate concentration range of 20% v/v. In one case, the leonardite char was activated with steam for 20 minutes followed by 3.5% v/v oxygen in nitrogen for an additional 5 minutes.

The activated carbons were characterized by TGA proximate analysis, SO₂ sorption in argon at ambient temperature and at 100°C, iodine number, surface area, and pore volume analysis.

RESULTS AND DISCUSSION

Deminerallization of the leonardite reduced the mineral matter to 6.8 wt% on a moisture-free basis with HCl and to 0.4 wt% moisture-free with HF. The proximate analyses of the raw, cleaned, and carbonized leonardite, as a function of carbonization and activation temperatures, are shown in Table 1 along with proximate analysis data for the carbonized lignite. Overall ash levels remain approximately constant with activation temperature for the uncleaned leonardite carbonized at 480°C and steam activated at temperatures of 700°C and above. As expected, volatile matter decreases with increasing activation temperature.

X-ray fluorescence analysis of the leonardite ash revealed that silicon, aluminum, and calcium are the major components, making up around 72 wt% on an oxygen-free basis, but the total weight of these four elements in the leonardite is 10.6 wt% as a consequence of the significantly high mineral matter

content (28.3 wt%) of the feedstock. The presence of calcium may be detrimental in the activation process for achieving microporosity but could be beneficial for assisting in the capture of SO₂.

A limited set of experiments was carried out on the lignite sample. Sorption tests with SO₂ at 100°C and 5000 ppm resulted in a small uptake, 2.4 wt% (g SO₂/100 g char) with fine carbon and 1.9 wt% with carbon pellets containing a binder, the carbons being produced in the TGA unit. Desorption at 100°C yielded a 0.2 and 0.4 wt% change, respectively, for the different samples, whereas desorption between 100° and 400°C yielded 1.0 and 0.9 wt% respectively.

Differences in sorption activity of products from the TGA and tube furnace reactor were seen in the case of the Georesources leonardite. Here the sorption activity was examined as a function of steam activation temperature for leonardite char carbonized at 480°C. Figures 1 and 2 show the SO₂ sorption data for ambient and 100°C conditions, respectively. The dependence of sorption activity on reactor type is less marked at the higher sorption temperature where the sorption capacity of the tube furnace product approached that of the TGA product. Reactor conditions would seem to affect significantly the resultant sorption activity where mass flow fields are appreciably different. The maximum sorption activity at ambient temperature and 100°C appears to occur for char activated between 750° and 800°C (6.1 and 6.8 wt% SO₂, respectively, at ambient temperature). However, the sorption activity is about one-third lower at 100°C (2.3 and 2.4 wt% SO₂, respectively,) than that at ambient temperature.

Owing to the similarity between the trends in Figures 1 and 2, it is feasible to plot the ratio of the two sorption values at the two sorption temperatures against activation temperature, as illustrated in Figure 3. The observed linear relationship leads to the following expression:

$$\%_{\text{Amb}}\text{SO}_2 = 2.79 \times \%_{100^\circ\text{C}}\text{SO}_2$$

Differences between the sorption activity at the two temperatures can be explained by the weakness of the physisorption bonding (Van der Waals) and the decline in relative strength between the Van der Waal's bond and the increasing vibrational component of the bond energy with increasing thermal energy.

The iodine number provides an alternative measure of sorption activity, the results of which are depicted in Figure 4 for the range of activation temperatures examined. Here it is seen more sharply that the optimum activation temperature for uncleaned leonardite char produced at 480°C is 750° to 800°C, corresponding to the SO₂ sorption results at 100°C (see Figure 2). However, the maximum iodine number of 460 mg I₂/g char (590 mg I₂/g C) is at the lower end of the range of that reported (600 to 1450 mg I₂/g C) for a commercial carbon.

Preliminary investigations on optimizing the carbonization and activation of leonardite (uncleaned) show that the maximum sorption activity as measured by SO₂ (5000 and 10,000 ppm in argon at 100°C) to be as follows: carbonizing temperature: 350°C, activation temperature: 750°C, activation time: 20 minutes. The results are shown in Figure 5. Subsequent activation with 3.5% v/v oxygen in nitrogen for an additional 5 minutes reduced the sorption by approximately 17%. This result is presumably due to a lowering of the microporosity as a result of increased burnoff.

Improvements in sorption activity of leonardite were found through physical cleaning. Carbonizing the 1.4 and 1.6 Certi-grav float-sink fractions (10.9 and 7.8 wt% ash, respectively) at 480°C, activation temperature of 750°C, and activation time of 20 minutes yielded 10.9 and 10.1 wt% SO₂, respectively, at 10,000 ppm SO₂ in argon at ambient temperature. The uncleaned leonardite yielded about 20% less SO₂ sorption (8.4 wt%).

Chemical cleaning of leonardite did not lead to successful sorption of SO₂ since both the HCl and HF severely modified the carbon matrix by removing the bridging divalent ions. The remaining gel-like carbonaceous material after carbonizing and activation yielded sorption data that were comparable to that determined for the carbons derived from the uncleaned leonardite. The behavior of acid-washed leonardite is significantly different from that of acid-washed lignite, as determined from our study of chemically cleaned lignite.

The surface areas, determined by N₂ multipoint BET, for the uncleaned and physically cleaned (1.6 float-sink) leonardite char, both steam-activated at 750°C for 20 minutes, were 81.6 m²/g and 90.0 m²/g, respectively. Although physical cleaning enhances the surface area slightly, nonetheless, gasification of leonardite char appears to affect the development of the surface area significantly.

CONCLUSIONS

Enhanced sorption activity towards SO₂ was obtained with physically cleaned leonardite (< 7 wt% ash) activated carbon. The conditions for its production were as follows: carbonization temperature: 480°C, activation temperature: 750°C, activation time with steam: 20 minutes. The best sorption activity determined was 10.9 wt% SO₂ with 10,000 ppm SO₂ in an argon stream. The surface area of the physically cleaned leonardite was 90.0 m²/g. Optimization of these conditions is expected to enhance the adsorptivity of the char significantly.

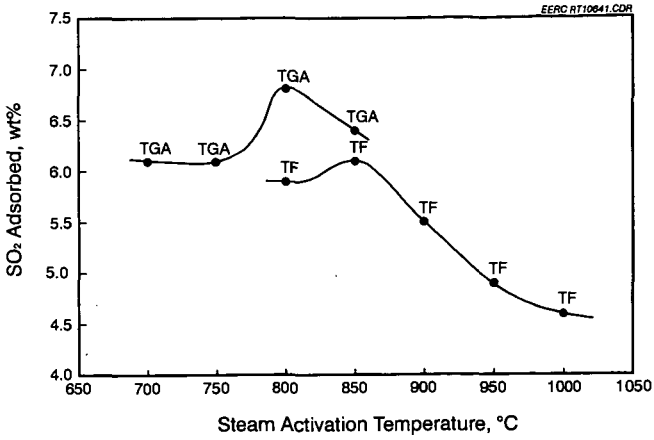


Figure 1. Dependence on activation temperature of SO₂ adsorption from flowing gas containing 5000 ppm SO₂ in argon at ambient temperature for Georesources leonardite (480°C) char.

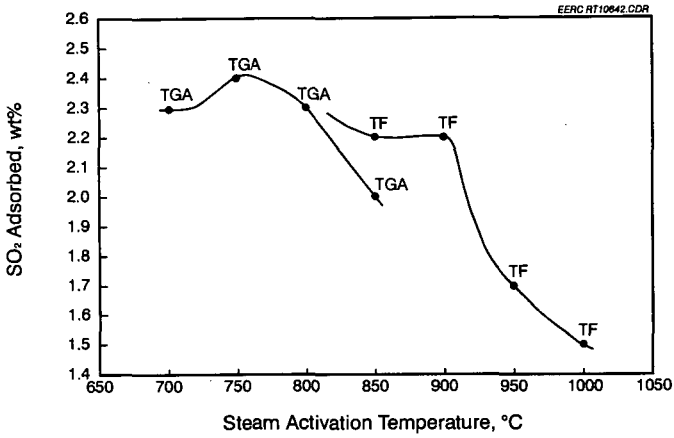


Figure 2. Dependence on activation temperature of leonardite SO₂ adsorption from 5000 ppm SO₂ in argon at 100°C for leonardite (480°C) char.

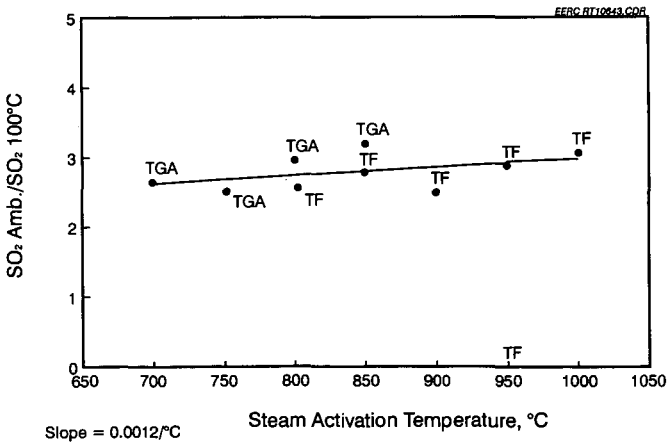


Figure 3. Ratio of SO₂ sorption capacity at ambient temperature to sorption capacity at 100°C for leonardite (480°C) char versus steam activation temperature.

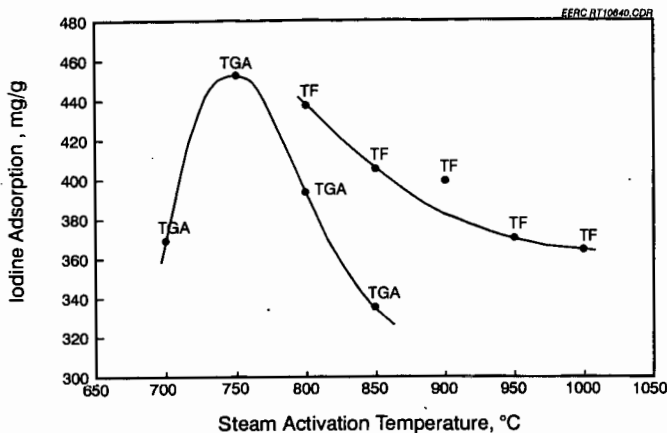


Figure 4. Sorptive capacity for I_2 of uncleaned leonardite (480°C) char steam activated at increasing temperatures.

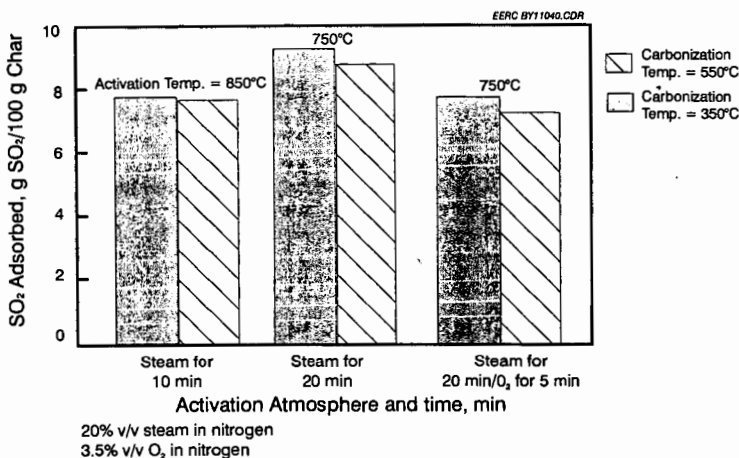


Figure 5. Effect of carbonization temperature and activation gas on SO_2 (10,000 ppm) adsorption at ambient temperature for leonardite chars.

REFERENCES

1. Wilson, J. *Fuel* 1981, 60, 823.
2. Samaras, P.; Diamadopoulos, E.; Sakellaropoulos, G.P. *Carbon* 1981, 29, 1181.
3. Bansal, R.C.; Donnet, J.-B.; Stoeckli, F. *Active Carbon*; Marcel Dekker: New York, 1988; p ix.
4. Samaras, P.; Diamadopoulos, E.; Sakellaropoulos, G.P. *Carbon* 1994, 32, 771.
5. Fernandez-Morales, I.; Lopez-Garzon, F.J.; Lopez-Peinado, A.; Moreno-Castilla, C.; Rivera-Utrilla, J. *Fuel* 1985, 64, 666.
6. Serio, M.A.; Solomon, P.R.; Basilakis, R. In *Proceedings of the International Conference on Coal Science*; Tokyo, Oct. 1989, pp 341-344.
7. King, A.J. *Chemical Society* 1937, 1489.
8. Boehm, H.P.; Heck, W.; Sappok, R. *Angewandte Chemie* 1984, 76, 742.
9. Voll, M.; Boehm, H.P. *Carbon* 1971, 9, 481.
10. Davini, P. *Carbon* 1993, 31, 47.
11. Knudson, C.L. "Leonardite Char Adsorbents," U.S. Patent No. 5 254 521, Oct. 19, 1993.

ACKNOWLEDGMENTS

The authors express their thanks to Mark Musich and Ron Kulas, both at the EERC, for their assistance in preparing the coals and chars and testing the carbons and to Georesources Inc. for supplying the leonardite. The authors also wish to extend gratitude to the U.S. Department of Energy Morgantown Energy Technology Center (METC) for financial support for this project.

PRODUCTION OF CHARCOAL AND ACTIVATED CARBON AT ELEVATED PRESSURE

Xiangfeng Dai, Niclas Norberg and Michael J. Antal, Jr.,
Hawaii Natural Energy Institute and the Department of Mechanical Engineering,
University of Hawaii at Manoa, Honolulu, HI 96822

Keywords: Biomass, Charcoal, Activated carbon

INTRODUCTION

With its wide range of properties, charcoal finds many commercial applications for domestic cooking, refining of metals (steel, copper, bronze, nickel, aluminum and electro-manganese), production of chemicals (carbon disulfide, calcium carbide, silicon carbide, sodium cyanide, carbon black, fireworks, gaseous chemicals, absorbents, soil conditioners and pharmaceuticals), as well as production of activated carbon and synthesis gas. In 1991, the world production of charcoal was 22.8 million cubic meters (3.8 million metric tons) (FAO, 1992) as shown in Table 1. Brazil is the world's largest charcoal producer---5.9 million cubic meters or one million metric tons was produced in 1991, most of which is used in steel and iron industry (Calle et al, 1992). African countries produced 45% of the world total amount of charcoal, where 86% of the wood-based energy is for domestic use (Khristova et al., 1993), most of which is inefficiently used. Charcoal is produced commercially in kilns with a 25% to 30% yield by mass on a 7 to 12 day operating cycle. Until recently, the highest yield of good quality charcoal reported in the literature was 38%.

Activated carbon has a wide range of applications, mostly as a purifying agent to remove trace quantities of undesirable species from gas or liquid phase, also as an economical media to recover materials. Some of the common applications are listed as follows: food industry, pharmaceutical industry, water purification, gas or air treatment, chemicals, oil refinery processing. Special applications of activated carbon are found in agriculture, as catalyst and catalyst support in chemical industry, for precious metal recovery and making batteries and military clothing, and in nuclear power stations. The consumption of activated carbon in industrialized countries in 1988 was 300,000 tons (Roskill, 1990), which was the majority of the world total. The United States and Japan account for 60% of this consumption---130,000 tons for U.S. and 50,000 tons for Japan. The yield of activated carbon produced commercially is low (typically 10% to 12%) from raw material.

In this paper, an ASME code rated experimental system is presented for producing charcoal and activated carbon from biomass feedstock. Very high yield of high quality charcoal is obtained in short cooking time, while very low yield of tar is found in the process from this system.

EXPERIMENTAL

Six biomass species were employed in this work, namely, Eucalyptus, Kiawe, Leucaena, Coconut husk, Macadamia nut shells and Kukui nut shells. All these feedstocks were air dried, the moisture contents of which are listed in Table 2. Macadamia nut shells and Kukui nut shells retained their original sizes of about 25 mm in diameter in hemispheric shape when being fed into the reactor. The other feedstocks were cut into small pieces (about 60 mm X 25 mm X 25 mm) in order to fit the feeding port of the reactor.

The experimental apparatus is schematically shown in Fig. 1. The reactor is made of 168 mm diameter X 1200 mm long steel pipe welded with flanges on both ends. A 114 mm diameter stainless steel canister is used to load feedstocks and to unload the reaction products. The available volume of the canister is 7.5 liters (2 gallons). The internal heating source consists of two 4 kW electric heaters, which are mounted on the bottom flange of the reactor. The heaters are controlled by a temperature controller. The Watt-hour meter is used to measure the power consumption. A back pressure regulator controls the reactor pressure. Thermocouples are placed in the center line of the reactor for measuring the temperature profile of the biomass bed. The effluents are flared in an exhaust line. For production of activated carbon by a thermal activation process, a steam and air mixture is used. The steam generator is built to provide a maximum steam flow of 3 kg/hr at 5.4 MPa pressure. Air is provided by an air tank with flow rate of 4 kg/hr. The whole system is ASME code rated---a "State Special" unit, which is operated with permission of the Hawaii State Boiler Inspector.

Feedstock is manually fed into the reactor. The experiment terminates when temperature or pressure remains stable or after a second temperature rise is observed. The heating time is about 3 hours from cold start. A tar converter is placed at the exit port. Charcoal and feedstock are analyzed according to ASTM standards by Huffman Laboratory, INC. The heat contents of Kukui nut shells and Kiawe are assumed 22 MJ/kg, which are conservatively estimated according to data of Macadamia nut shells and of Redwood (heartwood), respectively. The heat content of Eucalyptus (*Grandis*) is obtained using the following equation (Graboski et al., 1981):

$$\text{HHV} = 2.3236[(141\text{C} + 615\text{H} - 10.2\text{N} + 39.95\text{S}) - (1\text{-ASH})(17244\text{H/C}) + 149] \quad (\text{kJ/kg})$$

where HHV is the higher heating value on a dry basis, and C, H, N, S, ASH are the weight percent of carbon, hydrogen, nitrogen, sulfur and ash in the sample. Gas samples are analyzed using a gas chromatograph equipped with flame ionization and thermal conductivity detectors.

RESULTS AND DISCUSSIONS

The mass yield of charcoal is the ratio of dry charcoal to dry feedstock by mass. In Table 2 are shown the experimental results for mass yields of charcoal. All these species give very high mass yield---from 42% to 65%. The nut shells have higher mass yield than these wood species probably due to their higher fixed carbon content. For example, Macadamia nut shells has 23.7% fixed carbon content, while Eucalyptus (Grandis) 16.9% (Jenkins, 1989). Nevertheless, the mass yields of charcoal from these feedstocks are much higher than that produced from commercial kilns.

The energy yield, the ratio of heat content of dry charcoal to that of dry feed, is another indication of charcoal conversion. In Table 2 are also listed the energy yields of these charcoals. All of these give very high energy yield ranging from at least 64% to more than 88%.

The results of charcoal analysis are shown in Table 3. Samples for analysis are obtained from two extreme positions inside the reactor. Therefore, two sets of data are listed in the table. Generally speaking, charcoal closer to the heaters has higher fixed carbon (FC) content and higher heat content. Most of the charcoals have FC content and heating value lower than or close to British standard. However, after looking at the data from the previous work (Dai, 1993) which have higher FC content and heating value as well as very high mass yield, we conclude that the quality of these charcoals can be improved by a somewhat higher temperature cook. (This work is now in progress.) Moreover, Macadamia nut shell charcoal has FC content close to and heating value higher than British standard. Nevertheless, all these charcoals have higher FC content and higher heat content than commercial briquette charcoal, which implies that they are suitable for domestic cooking and their precursors are suitable raw materials for charcoal production.

Charcoal density is low due to its high porosity, which implies that charcoal is reactive and good for further pore development by activation process to make activated carbon. The bulk densities of charcoal are in the range of 45% to 65% of their raw materials. The bulk densities of Macadamia nut shells and Kukui nut shells are about 470 kg/m³ and 510 kg/m³, respectively. The shells sink in water.

From the temperature profiles in these experiments, it is found that under the reaction conditions, hemicellulose exothermicity occurs at about 275°C and cellulose exothermicity at about 350°C.

The result of gas analysis shows that the main gas species are H₂O, CO, CO₂, H₂ and CH₄. Other hydrocarbons are negligible. The typical molar ratio of CH₄, CO and CO₂ to H₂ is 1.7, 1.7 and 4.9.

Tar yield is very low, which reflects success of the reactor design and the tar converter. This also contributes to the high yield of charcoal.

Unfortunately, activated carbon production is now in process, and no information is available at this time.

CONCLUSION

Charcoal with very high yields of 42% to 65% has been produced from six biomass species in the newly built ASME code rated charcoal reactor. The nature of the feedstocks affect the yield and quality of charcoal significantly---the nut shells give higher yield and heat content of charcoal than wood species. Very low yield of tar is obtained in the process. Further work is now in progress to improve the uniformity of charcoal throughout the bed and to improve the quality of charcoal in terms of FC content and heating value while keeping mass yield still high.

REFERENCES

- Calle, F. R., Furtado, P., Hall, D. O. "Brazil charcoal: a case study for sustainable production and use". *Biomass Users Network*. July-Aug., 1992.
- Dai, X. "Charcoal production and gasification under pressure". MS thesis, May, 1993.
- Food and Agriculture Organization of the United Nation, *FAO Quarterly Bulletin of Statistics*, Vol. 5, No. 4 1992.
- Jenkins, B. M. "Physical properties of biomass". *Biomass handbook*. 1989.
- Khristova, P., Vergnet, L. "Evaluation of usher wood and karkadeh stem for charcoal in Sudan". *Biomass and Bioenergy*. Vol. 4, No.6, 455-459, 1993.
- Paddon, A. "Review of the available data concerning the amount of charcoal and fuelwood in Sudan". Field Project Document No. 22. FAO, Khartoum, 1987.
- Graboski, M., Bain, R. "Properties of biomass relevant to gasification". *Biomass gasification principle and technology*. Ed.: Reed, T. B., 1981.
- Roskill Information Services, Ltd. "The economics of activated carbon 1900". *PTS Research Studies*. 1-180. Aug. 9, 1990.

Table 1: The world annual production of charcoal for 1980 and 1991 (1000 cubic meter)

region	1980	1991
world	17117	22784
Africa	6883	10453
N. & C. America	821	904
S. America	6170	7480
Brazil	4779	5924

Table 2. Charcoal yields

Species	Mass yield (%)	Energy yield (%)	Feed moisture content(%)
Eucalyptus	46	67	15.7
Kiawe	53	>64	10.0
Leucaena	42*	66*	1.5*
Macadamia nut shells	51; 42*	76; 65*	13.5; 7.20*
Kukui nut shells	65; 62*	>84; >88*	12.1; 12.5*
Coconut husk	50	66	88.1

*data from the previous work (Dai, 1993).

Table 3. Charcoal evaluation

Species	Fixed carbon (%)	Volatile matter (%)	Ash (%)	HHV (MJ/kg)
Eucalyptus	53.1; 67.5	42.2; 30.9	4.66; 1.59	22.60; 28.62
Kiawe	57.4; 60.1	41.6; 30.9	0.95; 0.94	27.11; 26.08
Leucaena	67.6*	30.0*	2.34*	28.51*
Macadamia nut shells	68.9; 72.0	30.4; 27.1	0.74; 0.87	31.11; 31.74
Kukui nut shells	89.4*	9.37*	1.22*	32.43*
Coconut husk	52.3; 67.3	44.1; 29.2	3.55; 3.42	26.88; 29.71
Commercial briquette	46.5	36.4	17.2	22.8
Commercial Kiawe	69.8	28.3	1.96	29.7
Commercial Mesquite	86.8	9.04	4.17	31.8
British Standard (Paddon, 1987)	>75	<20	<7.0	>30.0

a *data from the previous work (Dai, 1993);

b The two numbers indicate samples from top and bottom of the reactor, respectively.

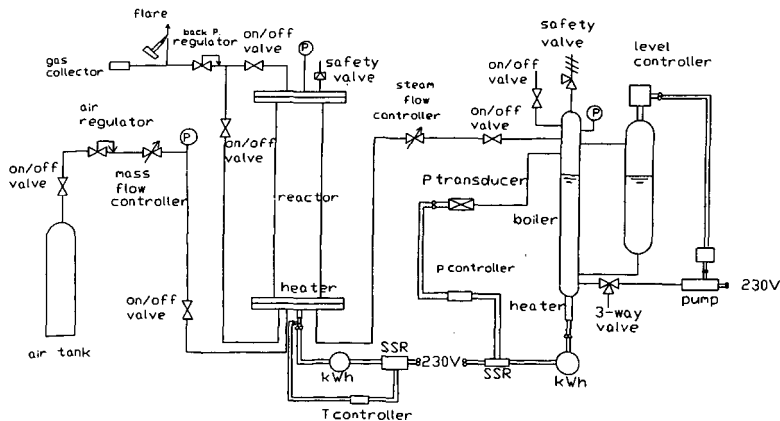


Fig. 1. Schematic diagram of the charcoal reactor

ACTIVATED CARBONS FROM STEAM EXPLODED WOOD.

Marit Jagtoyen, Frank Derbyshire, Robert S. Wright* and Wolfgang Glasser*
University of Kentucky, Center for Applied Energy Research,
Lexington, KY 40511-8433

*Biobased Materials Center, Virginia Polytechnical Institute,
Blacksburg, Virginia 24061-0323

Keywords: Activated carbon, Steam explosion, Porosity

INTRODUCTION

In a continuing experimental program, we are investigating the conversion of hardwoods, such as white oak (*Quercus alba*) to activated carbons by chemical activation with phosphoric acid¹⁻³. The aims of the research are to establish the relationships between chemical and morphological change and porosity development, with the long term goal of developing new adsorbents with controlled porosity and surface chemistry, through the selection of the precursor, reagent, and reaction parameters. The research is further directed to enhancing the use of wood materials, some of which are not appropriate feedstocks for conventional industrial applications, and to providing potential solutions to the problem of the economic utilization of wood wastes from primary and secondary wood industries.

Our previous work on phosphoric acid activation has demonstrated that there is a direct correspondence between porosity development and a dilation of the altered wood structure that takes place at heat treatment temperatures above about 200-250°C¹. While the mechanisms that lead to this structural expansion are unclear, it is clearly related to the effects of the reaction of phosphoric acid with the biopolymers in the wood, primarily lignin and cellulose. For example, compared to reaction in the absence of this reagent, phosphoric acid produces an increase in carbon yield that is attributed primarily to the retention of cellulose, albeit in altered form, through the promotion of crosslinking reactions. However, lignin and other biopolymers, also contribute to the pore structure. The most significant chemical changes seem to occur at low temperatures: ¹³C NMR spectra show that by 50°C there is a loss of carboxyl and methyl groups from the lignin structure, and the carbohydrate (cellulose and hemicellulose) signature disappears by 100°C⁴. These findings correspond with observations that lignin appears to undergo partial digestion or depolymerization at low temperatures¹. It has been reported in other work that wood transforms into a "plastic" state on heat treatment to low temperatures⁵.

For these reasons, current studies focus on elucidating the roles of wood biopolymers upon activation with H₃PO₄, and how they influence the porosity of the carbon product. In this context, wood and wood fractions have been produced by a technique known as steam explosion, that has been combined with extraction methods to provide materials with a range of different compositional characteristics for the synthesis of activated carbons. Steam explosion of lignocellulosic biomass from agricultural and forest resources is a technology that was developed for converting woody resources not qualified for the production of paper pulp into constitutive biopolymers⁶. The results presented here will consider how the pore size distribution of the activated carbons is influenced by the severity of the steam explosion treatment and fractionation protocol.

EXPERIMENTAL

Materials and Materials Preparation

Quantities of white oak were supplied in the form of wood chips (3 x 2 x 0.5 cm) by Westvaco Corporation. The chips were subjected to steam explosion treatment at four severity levels in a pilot scale unit at the Virginia Polytechnic Institute (VPI). Samples of the products were then subjected to solvent extraction to provide a total of 17 starting materials with different compositional characteristics: the parent wood; the complete steam exploded product at four severities, and extracted fractions from each of these - insoluble fractions from water and alkali extraction and recovered lignin from alkali extraction. A schematic of the steam explosion process and product separation scheme is shown in Figure 1.

The conditions used for steam explosion influence the chemical and molecular characteristics of the product and product fractions. A calculated severity parameter, log R₀, is used to denote the combined effects of time, temperature and steam pressure that are used in any particular treatment⁷. Differences in cell structure and in chemical structure are caused by varying the severity of steam explosion thus providing material of altered composition and microstructure.

Water extraction of the steam exploded wood fiber removes most of the hemicellulose. Alkali extraction creates a cellulose-rich fibrous fraction from which most of the lignin has been removed.

Extraction is accomplished using a liquor to wood ratio of 8:1, at a caustic charge of 15-20% of dry fiber, at 80 to 90°C for 30 minutes. Samples are then filtered, washed in a counter current mode and the solubles and insolubles are recovered. A lignin-rich fraction can be produced as a precipitate upon neutralization of the alkaline filtrate (approx. 90% lignin). By these procedures, the component biopolymers are isolated as xylose-rich water soluble solids; as cellulose-rich fiber solids; and as lignin-rich fraction by acid precipitation.

Chemical Activation

Activated carbons are synthesized by mixing an aqueous solution of phosphoric acid with the starting material, after first grinding the sample to produce a -100 mesh powder (to ensure good contact). The acid is added as an 85% solution in a volume such that the weight ratio of acid to as-received sample is 1.45 : 1.0. The mixture is then heat treated in two stages. First, low temperature heat treatment to 170°C for 30 min. under nitrogen flow to allow time for penetration of the reagent and to complete the initial reactions. This is followed by heating (again in flowing nitrogen) to a final temperature in the range 300-650°C, with a hold time of 1 hr. at maximum temperature. The product, after cooling, is then leached extensively with distilled water to pH 6-7 to recover the reagent, before drying and further characterization.

Characterization

Information on the carbon pore structure was derived from nitrogen adsorption isotherms obtained at 77K on a Coulter Omnisorb 100CX apparatus. Surface areas were determined by the BET method. Micropore volumes (pores less than 2 nm diameter), W_0 , were determined using the Dubinin-Raduskevich equation ⁸, and mesopore volumes (pores of diameter 2 to 50 nm diameter) were determined by the BJH method ⁹.

RESULTS AND DISCUSSION

One of the apparent effects of modifying the wood structure by steam explosion is that, compared to the parent wood, there is more visible evidence of reaction commencing at room temperature upon addition of the acid solution. This observation could be considered to be due to the opening of the wood structure by the steam explosion treatment, permitting increased access by the phosphoric acid. However, thermogravimetric analyses of samples of the parent wood and product from pretreatment at $\log R_0 = 4.0$ have failed so far to show any significant differences in behavior on H_3PO_4 activation.

The micropore and mesopore volumes of activated carbons produced from the parent wood and from samples subjected to steam explosion treatment at different severities (without subsequent fractionation) are shown in Figure 2, together with the totals of these volumes. It can be seen that, even at the lowest severity, steam explosion causes an appreciable increase in total pore volume (excluding macropores, defined as > 50 nm diameter). Compared to the parent wood, steam explosion at $\log R_0 = 4.0$ increases the total pore volume by about 30%. Most of this change is due to an increase in micropore volume, with an associated change in BET surface area from 1300 to 1950 $m^2 \cdot g^{-1}$, Figure 3. The result demonstrates that wood pretreatment by steam explosion can be very effective for producing structural changes that strongly influence the pore characteristics of the derived carbons.

As can be seen, with further increase in $\log R_0$ there is a progressive reduction in total pore volume, due to decreases in both micropore volume, as reflected by the changes in BET surface area shown in Figure 3, and in mesopore volume. The fact that the volumes in both pore ranges decrease together suggests that the effect of steam explosion severity on porosity is more complex than simply shifting the overall pore size distribution to larger or smaller pore sizes. It appears that, at high treatment severities, the wood structure is so extensively disrupted that the normal mechanisms by which phosphoric acid activation generates porosity begin to become appreciably impaired.

Further modifications to the steam exploded wood samples were effected by the solvent extraction scheme described earlier to produce: water-insoluble fractions; alkali-insoluble fractions; and lignin-rich fractions recovered from the alkali-solubles by precipitation. The pore structural parameters of activated carbons produced from these precursors, at the different levels of steam explosion severity, are summarized in Table 1: micropore volume, mesopore volume, and BET surface area - note that macroporosity is not included.

Although the reproducibility of these preliminary experiments has yet to be confirmed, certain trends can be tentatively identified. For the series of carbons produced from the water-insoluble fractions, the micropore volumes appear to be insensitive to $\log R_0$, over the range studied, while there is a reduction in mesopore volume with increasing severity. The alkali-insolubles produce carbons with lower microporosity, but here the mesopore volume increases with severity. The data indicate that mesoporosity passes through a maximum, but in any case very high mesopore

volumes have been measured at high severities. Carbons with these characteristics would be suitable for liquid phase applications, where wider pores are desirable from the standpoint of being able to accommodate large molecules, and to facilitate diffusion of the adsorbate through the liquid in the pores.

The lignin-rich fractions produced carbons with micropore volumes similar to those in the carbons from the alkali-insolubles, and again were unaffected by severity. However, the mesoporosity was reduced to low values at steam explosion severities greater than 4.0.

SYNOPSIS

The principal outcome of this research to date is that it has demonstrated that the techniques of steam explosion and solvent extraction allow the production of substantially different materials from a single wood type, and that these materials can function as precursors for the synthesis of powdered activated carbons possessing a range of pore structural characteristics. For example, low severity steam explosion can be used to increase the micropore volume and surface area and produce a carbon that would be more suitable for the adsorption of small molecules, typical requirements for gas phase adsorption. In contrast, high severity steam explosion followed by isolation of the alkali-insolubles can produce a carbon with high mesopore volume, suitable for liquid phase applications. The differences between these materials are clearly illustrated by the nitrogen adsorption isotherms in Figure 4: whereas adsorption on the predominantly microporous carbon approaches a plateau at a relative pressure above about 0.3, adsorption on the mesoporous carbon continues to rise due to the filling of wider pores.

In future work, further studies will be made to establish links between precursor composition and the properties of the powdered activated carbons, and investigations will be made of the feasibility of producing extruded activated carbons from these same precursors.

REFERENCES

1. M. Jagtoyen and F. Derbyshire, *Carbon*, **31** [7], 1993, 1185-1192.
2. M. Jagtoyen, F. Derbyshire, Proceedings CARBON'94, Granada, Spain, July 3-8, 1994, pp 232-233.
3. M. Jagtoyen, F. Derbyshire, W. Glasser, Proceedings CARBON'94, Granada, Spain, July 3-8, 1994, pp 228-229.
4. M. Solum, M. Jagtoyen, F. Derbyshire and R. Pugmire, accepted for publication, *Carbon*, 1995.
5. US Patent 5,238,470, 1993.
6. W. G. Glasser, B. K. Avellar, Symposium on Lignocellulosic Reactions-II. AIChE 1990 Spring National Meeting, March 11-12, Orlando, Florida, 1990.
7. R. P. Overend, E. Chornet, *Phil. Trans. R. Soc. Lond.*, **A 321**, 1987, 523-536.
8. Dubinin, M. M. Zaverina, E. D. and Raduskevich, *L. V. Zh. Fiz. Khimii*, 1351-1362, 1947.
9. E.P. Barrett, L. G. Joyner and P. H. Halenda, *J. Amer. Chem. Soc.*, **73**, 1951, 373.

ACKNOWLEDGEMENT

The authors would like to thank the US Department of Agriculture, Contract #93-02345, Program Director: Dr. Charles Cleland, and University of Kentucky, Center for Applied Energy Research for financial support.

Table 1: Micro- and mesopore volumes and BET surface areas of activated carbons from fractions of steam exploded wood.

Severity	Steam Exploded	Water Extracted	Alkali Extracted	Lignin
Micropore volume(cc/g) [*Parent wood 0.51 cc/g]				
4.01	0.77	0.76	0.60	0.56
4.26	0.67	0.73	0.42	0.58
4.35	0.7	0.75	0.44	0.59
4.43	0.59	0.77	0.60	0.57
Mesopore volume(cc/g) [*Parent wood 0.34 cc/g]				
4.01	0.36	0.41	0.21	0.56
4.26	0.44	0.26	0.45	0.13
4.35	0.26	0.22	1.07	0.14
4.43	0.25	0.18	0.69	0.17
BET surface area(m²/g) [*Parent wood 1300 m²/g]				
4.01	1945	1920	1408	1697
4.26	1589	1746	1166	1327
4.35	1691	1789	1314	1369
4.43	1413	1792	1734	1328

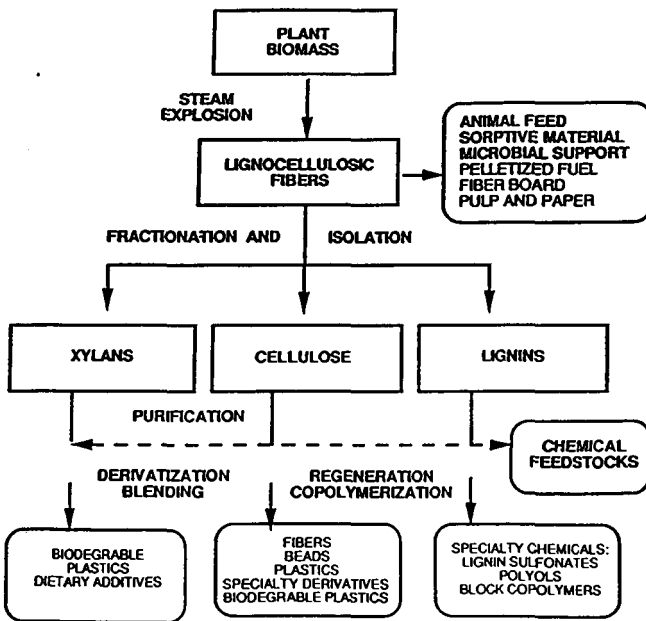


Figure 1: Schematic for separation of biomass into constituent polymers (Biobased Materials Center, Virginia Polytechnical Institute)

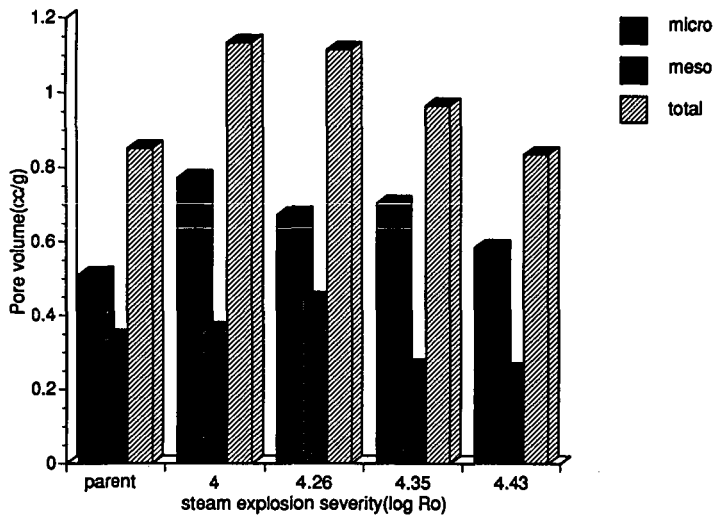


Figure 2: Influence of steam explosion severity on porosity of activated carbons (H_3PO_4 activation).

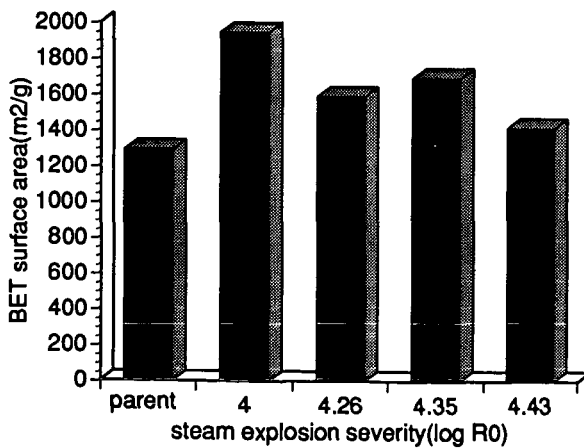


Figure 3. Influence of steam explosion severity on BET surface area of activated carbon (H_3PO_4 activation).

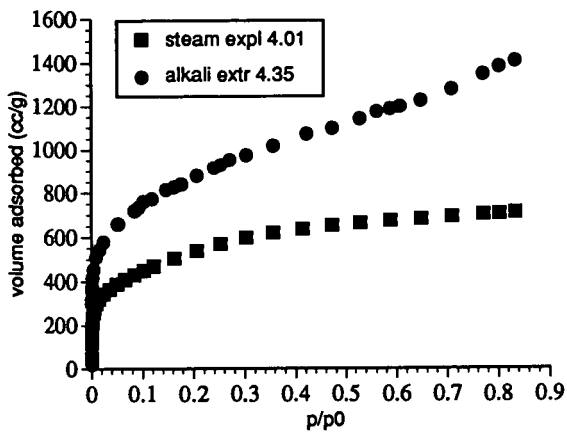


Figure 4. Nitrogen adsorption isotherms (77K) of activated carbons. (precursor materials derived from white oak)

X-RAY CHARACTERIZATION OF SOME ACTIVATED CARBON PREPARED FROM ILLINOIS BITUMINOUS COAL 106 AT THE CAER

David L. Wertz, Shuhua Jin, and Charles B. Smithhart*
Department of Chemistry & Biochemistry

and
Center for Coal Product Research
University of Southern Mississippi
Hattiesburg, MS 39406-5043 USA

Key Phrases: Activated carbon, x-ray spectroscopy, x-ray diffraction, phosphorus retention.

INTRODUCTION

X-ray fluorescence spectroscopy (XRS) has been an established research tool for at least seventy-five years for the elemental analysis of condensed phases. Because of recent advances in materials development for the transmission and collection of soft x-rays ($\lambda > 10 \text{ \AA}$), XRS offers new advantages in the study of fossil fuels and their processed products. Wavelength dispersive x-ray fluorescence spectroscopy offers the added advantages of a very low background and excellent peak length/width ratio. Taken together, these features allow WDXRS to be used for the detection of elements in condensed phases at the parts per million abundance level, and in some cases significantly lower.¹

With WDXRS, as well as many other types of radiation experiments, attenuation of the incident and secondary radiation beams by the sample occurs. The result is that the measured intensity I_{meas} cannot be related to sample abundance.²

The absorption-corrected intensity of a WDXRS peak, $I^0(\lambda_Q)$, is directly proportional to the abundance of analyte Q at λ_Q . $I^0(\lambda_Q)$ is related to the intensity measured at λ_Q by:

$$I^0(\lambda_Q) = [\alpha \cdot \Sigma w_A \cdot \mu_A(\lambda_p) + \beta \cdot \Sigma w_A \cdot \mu_A(\lambda_Q)] \cdot I_{\text{meas}}(\lambda_Q) \cdot [1 - \exp\{-\{\alpha \cdot \Sigma w_A \cdot \mu_A(\lambda_p) + \beta \cdot \Sigma w_A \cdot \mu_A(\lambda_Q)\}\}]. \quad (1)$$

In eq. 1, w_A represents the abundance of element A in the condensed phase sample, $I_{\text{meas}}(\lambda_Q)$ is the intensity measured at wavelength λ_Q due to the presence of analyte Q in the sample. The mass absorption coefficients, $\mu_A(\lambda_p)$ and $\mu_A(\lambda_Q)$, are for the attenuation (absorption) of the primary radiation (chromium in these experiments) and for the secondary radiation emitted by the analyte Q, respectively. Constants related to the mass of the sample are represented by α and β . The terms containing the absorption coefficients are designated the "matrix absorption" due to the sample and have a pronounced effect on the relationship between the measured intensity and the absorption-corrected intensity for analyte Q.

The condition of "infinite thinness" may be achieved when the matrix absorption effect $\rightarrow 0$ and is relatively constant. When this condition is satisfied, $w_Q = I_{\text{meas}}(\lambda_Q)/K'$; and the intensity of the peak at λ_Q provides a useful measure of the abundance of analyte Q. The condition of "infinite thinness" is achieved in cleaned coal and biomass samples, where the presence of metal atoms is quite small and the structural units are predominantly either hydrocarbons and/or carbohydrates.

EXPERIMENTAL

Samples were obtained from Jagtoyen as fine powders and were examined as received using conventional x-ray diffraction and x-ray spectral methods.

RESULTS AND DISCUSSION

As seen in Figure 1, the FeS_2 , Fe_2O_3 , SiO_2 and/or CaCO_3 (which are strong absorbers of Cu K_α X rays) had been successfully removed from the IBC 106 prior to its use.

Jagtoyen and Derbyshire have discussed the processes by which bituminous coals and hardwood have been treated by their high temperature (HTT) phosphoric acid process.^{3,4}

Shown in Figure 2 are the WDXRS spectra obtained from several samples of demineralized IBC 106 coal treated by the CAER hot phosphoric acid process used over the temperature range from ambient temperature (labeled DM coal) to 650°C. At ambient temperature a

large sulfur peak ($\lambda = 5.372 \text{ \AA}$) is noted, corresponding to an organo-sulfur abundance of ca. 2.1% in the cleaned coal. Comparison of the sulfur peak intensities indicates that as the process temperature is increased, the percentage of sulfur retained in the carbon fibers reduced. When processed at 650°C , the fibers retain ca. 0.4%. Accompanying the increase in process temperature is a retention of phosphorus ($\lambda = 6.155 \text{ \AA}$).

A similar increase in phosphorus retention is found in the white oak samples treated by Jagtoyen.^{3,4}

WDXRS cannot be extended to provide detailed information about the structural role(s) of the phosphoric acid species involved in the CAER process because the technique only provides elemental (and not molecular) information.

We have previously shown⁵ that the full-width at half maximum (FWHM) for the graphene stacking peak, found at $3.5\text{-}4.0 \text{ \AA}$ in bituminous coals, measures the regularity of the stacking of the graphene layers in coals. Shown in Figure 4 are the x-ray diffractograms (XRD's) obtained from the unprocessed IBM 106 coal and the coal processed at the several temperatures noted above. Comparison of the XRD's indicates that the FWHM of the graphene stacking are affected significantly by the process temperature, with the higher process temperatures causing improved regularity of the graphene peaks.

Shown in Figure 5 is evidence that the reduction in FWHM is not due to thermal effects.

Jagtoyen⁶ has measured the BET surface area of the activated carbon produced from the IBC 106 as a function of process temperature. In addition, the CAER team reports a significant reduction in the hydrogen component of the activated carbon produced by their HTT process.³ The increase in surface area and the reduction in hydrogen content parallel, at least crudely, with phosphorus uptake (measured by WDXRS) and the re-alignment of the graphene layers in the activated carbon (measured by XRD).

CONCLUSIONS

The two x-ray characterization methods, wavelength dispersive x-ray spectroscopy and x-ray diffraction, each provide limited information about carbon fibers prepared by Jagtoyen and Derbyshire. Unfortunately, neither method provides definitive information about the structural and/or bonding roles of the phosphorus moieties in the activated carbon.

REFERENCES

* Support via a DOE-EPSCoR Graduate Fellowship is gratefully acknowledged.

1. Jenkins, R., "X-Ray Spectrometry", John Wiley & Sons, NY, 1988.
2. Klug, H. and Alexander, L. E., "X-Ray Diffraction Procedures", Wiley-Interscience, NY, p. 360.
3. Toles, C., Rimmer, S. M., Derbyshire, F., and Jagtoyen, M., *Am. Chem. Soc., Div. Fuel Chem.*, 1994 (39) 596.
4. Jagtoyen, M. and Derbyshire, F. J., *Carbon*, 1993 (31) 1185.
5. Wertz, D. L. and Bissell, M., *Energy & Fuel*, 1994 (8) 613.
6. Jagtoyen, M., private correspondence.

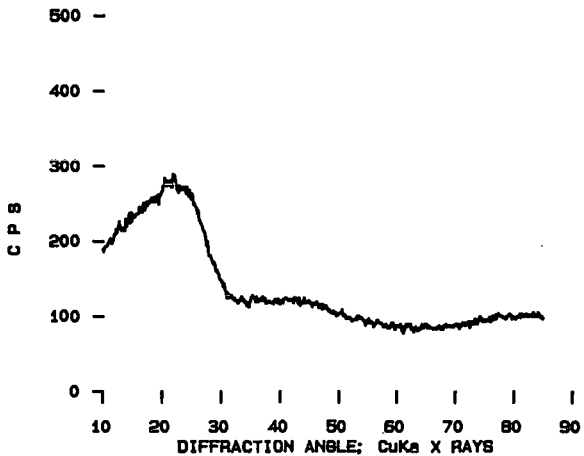


FIGURE 1. XRD OF THE CLEANED IBC 106.

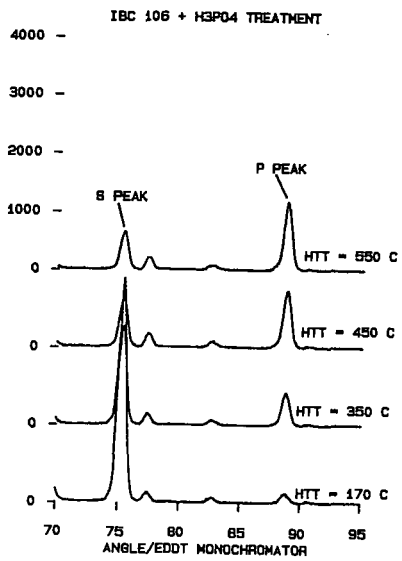


FIGURE 2. WAVELENGTH DISPERSIVE X-RAY SPECTRA OF THE IBC SAMPLES TREATED WITH THE KCAER HTT TREATMENT OVER THE RANGE FROM AMBIENT TO 550°C. SULFUR AND PHOSPHORUS PEAKS ARE LABELED.

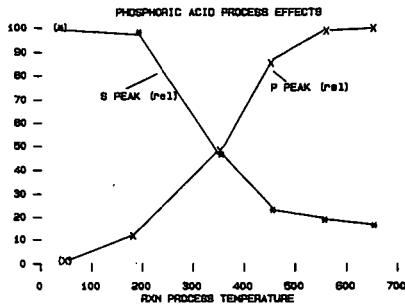


FIGURE 3. HTT EFFECTS ON ORGANO-SULFUR AND PHOSPHORUS UPTAKE.

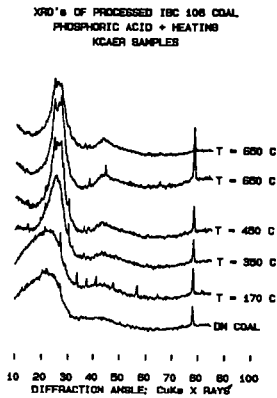


FIGURE 4. HTT EFFECTS ON THE XRD'S OF THE ACTIVATED CARBONS.

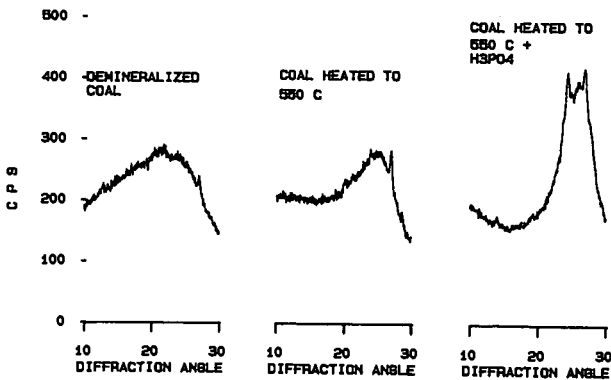


FIGURE 5. CORRELATION OF PHOSPHORUS RETENTION WITH BET SURFACE AREA⁶ MEASURED FOR THE ACTIVATED CARBONS.

PYROLYSIS AND HYDROLYSIS OF BIOMASS AND LIGNINS - ACTIVITIES AT THE INSTITUTE OF WOOD CHEMISTRY IN HAMBURG, GERMANY

Dietrich Meier, Jochem Berns and Oskar Faix
Federal Research Centre for Forestry and Forest Products
Institute of Wood Chemistry and Chemical Technology of Wood
21027 Hamburg, Germany

Keywords: biomass, lignin, hydrocracking, pyrolysis, liquefaction

INTRODUCTION

After the first oil price crisis in 1973 research activities were initiated throughout the world to produce oil from renewable feedstocks like lignocellulosic biomass. Countries with huge biomass resources and strong dependence on imported petroleum such as Canada and the United States of America were leading in research at that time. At the Pittsburgh Energy Research Center (PERC) high pressure liquefaction of cellulosic wastes was studied using carbon monoxide and sodium carbonate as a catalyst (1), and a pilot plant in Albany, Oregon was constructed. At the same time, another high pressure conversion process for woody biomass was investigated at the Lawrence Berkeley Laboratories (2). The scaled-up version of this process was also tested in Albany. After several years of operation, the pilot plant was shut down due to economical and technical reasons. It was felt that high pressure technology is too sophisticated for the thermal conversion of biomass into liquid fuels and that simpler technologies should be developed. Therefore, in 1980 the Solar Energy Research Institute (today NREL) in Golden, Colorado, organized a specialists' workshop on fast pyrolysis of biomass. This process promised to give high yields of liquid products. During the workshop, researchers working on coal and biomass presented papers on both fundamental aspects - such as heat transfer mechanisms - and practical work regarding process parameters such as feedstock, particle size, heating rate, residence time, pressure etc. Since the early eighties a lot of progress has been made in the development of conversion technologies for biomass. The most important processes with their characteristics are compiled in Table 1.

In 1982 the German government also recognized the need for using renewable feedstocks and funded a research project dealing with the direct conversion of wood into a liquid fuel and/or chemical feedstocks. Based on the large tradition and experiences in coal conversion by the high pressure Bergius-Pier process in Germany (14 plants produced all transportation fuels during World War II) the Institute of Wood Chemistry (IWC) adopted the process principles to woody feedstocks. During several years of experimental work at IWC, various process alternatives were studied covering

- slurry phase hydrocracking in batch and semi-continuous reactors
- hydrolysis in batch and semi-continuous reactors
- flash pyrolysis in a bench-scale fluidized bed reactor.

In the present paper the research activities and main results on thermochemical conversion of biomass and lignins are summarized.

HIGH PRESSURE EXPERIMENTS

Initial hydrocracking experiments were conducted in 25 ml autoclaves to compare conversion rates of different lignocellulosic feedstocks and to develop methods for separation and chemical characterization of the liquids (3, 4). Palladium on active charcoal (Pd/C) was initially used as a catalyst. Temperature was 475°C and initial hydrogen pressure 6 Mpa. Surprisingly, very small amounts of solid residue ranging from 0.5 to 6.8 % were observed for all kinds of biomass such as softwood, hardwood, straw, sugar cane bagasse, lignins and cellulose. The oil

yields of the lignocelluloses were in the range of 41 %. Cellulose and hemicelluloses gave rise to around 30 % and lignins to ca. 62 % of an oil. The average molecular weight of the oil was around 500 Dalton indicating severe depolymerization of the feedstocks during hydrocracking. The mass balance of these studies demonstrated that lignin is a more suitable feedstock with respect to oil yields than cellulose and hemicelluloses which have a tendency to give more char, water and gas.

After these orienting studies with the micro-autoclaves, experimental work was continued including a 1-L autoclave system (see Figure 1).

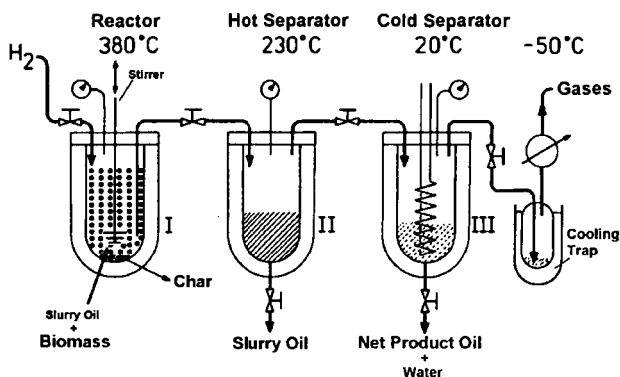


Fig. 1-L autoclave system for hydrocracking of biomass

It consists of a high pressure stirred reactor, a high pressure hot separator and a high pressure cold separator (5). A slurry phase catalytic hydrocracking process was developed with Pd/C as catalyst. In general, spruce wood particles were mixed with the high boiling recycle oil fraction which was condensed in the hot separator at 230 °C. The light and middle distillate fraction was collected in the cold separator and yielded around 37 % of a net product oil (NPO). Several consecutive runs were made in which always the hot separator fraction of the previous run was used as a slurry oil. In this way, the stability of the recycled oil was proved and the conditions of a continuous process could be simulated. The experiments revealed that the NPO yields and the amount of recovered recycle oil were almost constant in all runs. Therefore, a mass balance was established which reflects the overall yields of each product fraction from hydrocracking of biomass (Figure 2).

Beside palladium, other catalysts were included in the hydrocracking experiments such as Co, Mo, Cr, Ni, Fe, and red mud. However, none of these catalysts reached the NPO yields of palladium. The slurry oil could be completely recycled only in the presence of the iron catalyst and a NPO yield of 28 % was found. In general, the NPO's had a heating value of around 37 MJ/kg. An energy balance for the hydrocracking conversion process is presented in Figure 3, taking into account a hydrogen consumption of 4 % and the individual proportions and heating values of the biomass constituents. The balance demonstrates that 59 % of the input energy can be recovered and concentrated in the NPO. Its light fraction amounted to 50 % having a boiling point range < 220°C. The rest could be completely distilled between 220-360°C. In

comparison to oils obtained in the Albany plant, the NPO had a very low viscosity of 3.88 cSt at 20°C, a low pour point of -24°C, and a low density of 0.92 g/l (6).

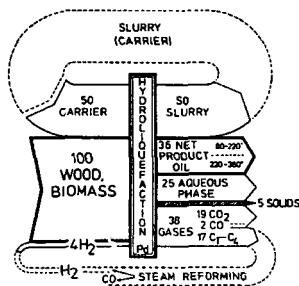


Figure 2 Mass balance for hydrocracking of biomass

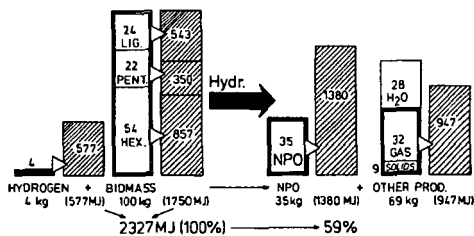


Figure 3 Energy Balance for hydrocracking of biomass

The variation of process parameters was also studied and is documented in various publications (7-9). There is a positive correlation between the pressure and the yield of liquids and a negative correlation between the pressure and the amount of char. At 3 MP initial hydrogen pressure the char yield is as high as 40 % but between 10 and 13 MPa, char formation is very low and amounts to ca. 5 % (8) (see Figure 4). The chemical characterization of the NPO's was mainly done by capillary gas chromatography and mass spectrometry with special emphasis on the qualitative and quantitative determination of phenolics which industry is mostly interested in. However, the unambiguous assignments of reaction products was difficult for the slurry oil phase reactions because the recycling oil was also degraded to a certain extent.

Therefore, we carried out hydropyrolysis experiments without a co-solvent using the same conditions as before in the hydrocracking experiments. Beside spruce wood and china grass, we also included technical lignins from various pulping processes as feedstocks in our experimental designs. Conversion of the feedstocks was excellent (10-12). In some cases, at suitable conditions, no char was formed. In general, lignins gave very high liquid yields of up to 80 %. VEBA OEL, the largest German refinery company, showed interest in lignin

hydrocracking for phenol production as methyl-aryl-ethers can be used as octane enhancers in gasoline. For this reason, we concentrated our work on lignin. A lot of experiments were performed at IWC including the application of slurry oils derived from petroleum and lignin. Despite of the high conversion rates, the amount of mono-phenols did not come up to our expectations. In the best case the yield of monomeric phenols was around 13 wt% (13,14).

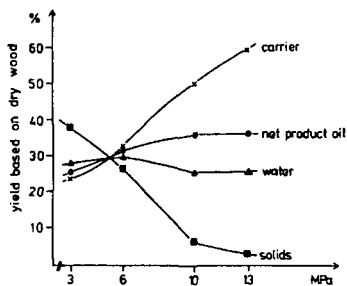


Figure 4 Yield of hydrocracking products at different initial hydrogen pressures

FLASH PYROLYSIS OF BIOMASS IN A FLUIDIZED-BED REACTOR

Since the aforementioned workshop on flash pyrolysis, several technologies have been developed mainly in Canada and the United States. At the moment, the most advanced flash pyrolysis technologies available are from ENSYSN, Gloucester, Ontario, Canada, (circulating fluidized bed), the University of Waterloo, Waterloo, Canada, (stationary fluidized bed) and NREL, Golden, Colorado, USA (vortex reactor). The Canadian know-how is now being exported to Europe. Especially the Waterloo Fast Pyrolysis Process (WFPP) is applied in research laboratories in Spain, Great Britain, Finland, and Germany. The first pilot plant of the WFPP process, with a capacity of 200 kg/h, was installed in Spain funded by the EU and UNION FENOSA, a Spanish energy producer. Another pilot plant from ENSYN, Canada, will be erected in Italy in 1995. A typical mass balance of the flash pyrolysis process is shown in Figure 5. The elemental composition of the liquids is very similar to wood. Their quality is quite different from high pressure oils. They contain water (10 to 35 %) and are rich in oxygenated compounds. Pyrolysis liquids are corrosive due to their low pH-value and thermally unstable because they tend to condensate at elevated temperatures. Therefore, the direct use is difficult and upgrading is necessary depending on the application.

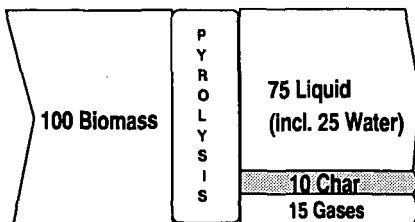


Figure 5 Mass balance of flash pyrolysis

Recently, the investigations on thermochemical conversion at IWC were also extended to flash pyrolysis using a continuously operating bench scale fluidized-bed reactor from the University

of Waterloo with a capacity of 100 g/h. A reactor description is given elsewhere (15). There are several reasons why fast pyrolysis is now so attractive:

1. There is an increased interest in the EU to produce biofuels by flash pyrolysis for the production of power, transportation fuels, and chemicals.
2. ICW is involved in a EU research project on "Integrated Chemicals and Fuels Recovery from Pyrolysis Liquids Generated by Ablative Pyrolysis". Within this project we can use our expertise in analysis, fractionation, and upgrading of bio-oils.
3. IWC got funds from the German Foundation for Environment to investigate the possibilities of using the flash pyrolysis technology for the disposal of contaminated wood waste.

For this purpose a 1 kg/h pilot plant with a fluidized bed reactor and gas recycling will be erected at IWC in 1995. Flash pyrolysis in fluidized beds has some advantages over conventional incineration of waste wood which actually in Germany is very limited due to legislative restrictions. (1) the gas volume in the process is drastically reduced. Thus, gas cleaning is more easier, (2) the formation of dioxins is unlikely to occur due to the absence of oxygen, (3) the plant capacity can be very small.

REFERENCES

1. Appell, H.R., Y.C. Fu, E. G. Illig, F.W. Steffgen and R.D. Miller (1975) Bureau of Mines, Report of Investigation 8013, Pittsburg.
2. Elliott, D.C., *Biotech. & Bioeng. Symp. No. 11* (1981), 187-198.
3. Meier, D., D.R. Larimer and O. Faix (1986) *Fuel*, 65, 910-915.
4. Meier, D., D.R. Larimer and O. Faix (1986) *Fuel*, 65, 916-921.
5. Meier, D, K. Fuch and O. Faix (1987) "Energy Biomass & Wastes X", 785-800.
6. Meier, D. and O. Faix (1988) "Research in Thermochemical Biomass Conversion" (eds.: Bridgwater, A.V, J.L.Kuester) Elsevier, 804-815.
7. Meier, D., L. Jakobi and O. Faix (1988) *J. Wood Chem. Techn.*, 8, 523-542.
8. Meier, D. and O. Faix (1989) "Energy from Biomass 4" (eds.: G. Grassi, D. Pirrwitz, H. Zibetta) Elsevier, 584-592.
9. Meier, D. and M. Rupp (1991) "Biomass Pyrolysis Liquids Upgrading and Utilization" (eds.: A.V. Bridgwater, G. Grassi) Elsevier, 93-102.
10. Meier, D. and O. Faix (1990) "Biomass for Energy and Industry 5", Vol. 2, (eds.: G. Grassi, G. Gosse, G. dos Santos) Elsevier, 2646-2650.
11. Meier, D. R. Ante and O. Faix (1992) *Bioresource Technol.*, 40, 171-177.
12. Oasmaa, A. R. Alén and D. Meier (1993) *Bioresource Technol.*, 45, 189-194.
13. Meier, D. J. Berns and O. Faix (1994) "Advances in Thermochemical Biomass Conversion (ed.: A.V. Bridgwater) Blackie, Vol.2, 1016-1031.
14. D. Meier, J. Berns, O. Faix, U. Balfanz and W. Baldauf (1994) *Biomass & Bioenergy* (in press)
15. Scott, D.S. and J. Piskorz (1984) *Can. J. Chem. Eng.*, 62, 404-412.

Table 1 Main processes and characteristics for the thermal conversion of biomass

Technology	Main characteristic	Catalyst	Temperature (°C)	Pressure (bar)	Residence time	Main primary products, application, comments
Combustion	O ₂ /air in excess	N	ca. 1000	N	short	heat
Gasification	O ₂ /air limited (also with steam)	Y/N	1000-1500	Y/N	short	synthesis gas, fuel gas, ethene, ethin, ... "I C chemistry" ... "indirect liquefaction"
Pyrolysis	inert gas atmosph.	N	> 450	Y/N	very long (hrs, days)	charcoal (carbonisation)
Pyrolysis	inert gas	N	>450	N	short (> min)	fuel gas, liquid tar (low yield), solid char
Pyrolysis	inert gas	N	>450	N	very short (< sec)	(flash pyrolysis) aqueous, acidic liquid tar for fuel (high O content) and chemicals
Pyrolysis	inert gas	Y	various	reaction conditions	various	catalytic pyrolysis under development
Liquefaction	CO (H ₂) in H ₂ O/alkali	Y	350-400	300	>15min	sometimes in combination with pretreatments, O content of liquids is still high
Hydro-pyrolysis	H ₂ atmosph. (gas/solid phase)	Y	350-600	50-200	>15 min	low viscous oil in high yield, low O content
Hydro-cracking	H ₂ atmosph. (gas/liquid phase)	Y	350-450	50-200	>15 min	low viscous oil in high yield, low O content
Hydro-treating	H ₂ atmosph. (gas phase)	Y	various	reaction conditions	various	used for upgrading of pyrolysis oils, O content below 1 %

CATALYTIC GASIFICATION OF WET BIOMASS IN SUPERCRITICAL WATER

Michael J. Antal, Jr., Yukihiko Matsumura, Xiaodong Xu, Jonny Stenberg, and Peter Lipnik
Hawaii Natural Energy Institute and the Department of Mechanical Engineering,
University of Hawaii at Manoa, Honolulu, HI 96822

Keywords: Wet biomass, Catalytic gasification, Supercritical water

INTRODUCTION

Wet biomass (water hyacinth, banana trees, cattails, green algae, kelp, etc.) grows rapidly and abundantly around the world. As a biomass crop, aquatic species are particularly attractive because their cultivation does not compete with land-based agricultural activities designed to produce food for consumption or export. However, wet biomass is not regarded as a promising feed for conventional thermochemical conversion processes because the cost associated with drying it is too high. This research seeks to address this problem by employing water as the gasification medium. Prior work has shown that low concentrations of glucose (a model compound for whole biomass) can be completely gasified in supercritical water at 600°C and 34.5 MPa after a 30 s reaction time (Dehui et al., 1993). Higher concentrations of glucose (up to 22% by weight in water) resulted in incomplete conversion under these conditions. The gas contained hydrogen, carbon dioxide, carbon monoxide, methane, ethane, propane, and traces of other hydrocarbons. The carbon monoxide and hydrocarbons are easily converted to hydrogen by commercial technology available in most refineries. This prior work utilized capillary tube reactors with no catalyst. A larger reactor system was fabricated and the heterogeneous catalytic gasification of glucose and wet biomass slurry of higher concentration was studied to attain higher conversions.

EXPERIMENTAL

A schematic drawing of the reactor system is presented in Figure 1. The reactor was constructed of Inconel 625 tubing with a 0.375" OD and 0.187" ID. The temperature of the reactant flow was abruptly raised to a desired value using an entry heater/cooling water jacket combination. The reactor was maintained at isothermal conditions using a furnace and downstream heater/cooling water jacket combination. To improve the heat transfer from the heaters to the fluids inside the reactor, the heaters were coiled on stainless steel rods in direct contact with the Inconel reactor. Different amounts of solid catalyst could be packed inside the reactor, giving the desired weight hourly space velocity (WHSV), which is defined as the ratio of the mass flow rate of the reactant to the mass of a proprietary "catalyst X" used in the heated zone. The axial temperature profile along the reactor's functional length of approximately 0.48 m was measured with 15 fixed, type K thermocouples. Pressure in the reactor system was measured using a pressure transducer. A back pressure regulator reduced the working pressure from 34.5 MPa to atmospheric pressure. After passing through the back pressure regulator, the reactor effluent then passed through an in-house fabricated glass gas-liquid separator. The gas flow rate was measured using a wet test meter.

The aqueous solution of glucose was fed into the reactor by an HPLC pump. A balloon feeding system was employed to feed the wet biomass slurry. Wet biomass was first ground with a blender and then with a homogenizer. The heterogeneous biomass slurry filled the 500 ml high pressure/temperature vessel, which was equipped with a magnetic drive. A meteorological balloon was placed in the vessel together with the biomass slurry. Water was pumped into the balloon, and as the balloon expanded the biomass slurry was forced into the reactor.

The analysis of the gaseous products was accomplished on a gas chromatograph equipped with flame ionization and thermal conductivity detectors. A 800/100 mesh carbosphere molecular sieve packed column was used, operating at 35°C for 4.2 min, followed by a 15°C/min ramp to 227°C, a 70°C/min ramp to 350°C, and a 5.3 min hold at 350°C. The following gases were detected as the products of glucose gasification: H₂, CO, CO₂, CH₄, C₂H₄, C₂H₆, C₃H₆, and C₃H₈. Gas yields were calculated as the ratio of mole of detected gas to the mole of reactant. Carbon gasification efficiency was calculated as the ratio of carbon converted into gas.

Ten cubic centimeters of the liquid effluent from the experiments were dried in small beakers in an oven and the weight gain measured. A dark tar deposit remained on the bottom of the beaker after the drying for lower temperature or higher concentration. Tar yield was calculated as the ratio of the weight of tar to the weight of the reactant.

RESULTS AND DISCUSSIONS

1. Temperature effect

The effect of temperature on the gasification of glucose in the presence of catalyst X is shown in Table 1. Complete carbon conversion was observed at 600°C; however, as temperature dropped, carbon gasification efficiency decreased drastically. When the reaction temperature was

below 580°C, resulting in incomplete gasification conversion, the liquid effluent became yellowish and there was a thin layer of a dark brown, oil-like tar. Figure 2 illustrates the amount of tar present in the liquid sample as a function of reaction temperature. It is obvious that the tar yield in the liquid sample increases as temperature decreases. The tar yield at 600°C is significantly small.

2. Reactant concentration effect

When 0.2 M glucose was gasified without the solid catalyst X at about 30 s residence time in supercritical water at 600°C, 34.5 MPa, complete carbon conversion was observed. The liquid sample was clear. As the reactant glucose concentration increased, the carbon conversion decreased. With 0.8 M glucose reactant, the conversion dropped to 88%, and a dark brownish oil layer was present in the liquid sample.

The presence of solid catalyst X resulted in complete conversion of glucose feed with concentration as high as 1.2 M at a WHSV of 22.2 (g/h)/g (see Table 2). The liquid effluent was clear. Gas yields of H₂, CO, CH₄, and CO₂ increased significantly with the addition of catalyst X.

3. Pressure effect

When the pressure increased from 25.6 MPa to 34.5 MPa, the overall carbon gasification efficiency remained almost the same. However, as pressure increased, the yield of methane increased. This finding confirms the results of Elliott et al. (Elliott et al., 1993a, 1993b; Baker et al., 1989; Sealock et al., 1993).

4. Deactivation of catalyst

Deactivation of catalyst was observed in an 8-hour experiment using 1.2 M glucose as a reactant. As shown in Table 3, the carbon gasification efficiency decreased, while the solid residual and carbon content in the liquid sample increased with time.

The liquid samples were collected for total organic carbon (TOC) analysis. TOC yield was calculated as the weight ratio of carbon in the liquid effluent to that in the reactant. Because of the lower carbon gasification efficiency, more carbon remained in the liquid effluent at the later stage of the experiment, as indicated in Table 3. Notice that the tar yield (which is a measurement of the non-volatile residual in the liquid effluent) also increased with time.

5. Whole biomass gasification

Various whole biomass feeds, including water hyacinth, depithed bagasse liquid extract, sewage sludge, and paper sludge, were studied in the packed bed reactor. The gasification of the above feeds with catalyst X at 600°C, 34.5 MPa, resulted in a complete conversion to gas. The gas contained H₂, CO₂, CH₄, and trace amounts of high hydrocarbons. The amount of carbon monoxide in the gaseous product mixture was very small. Virtually no tar or char products were detected by the evaporation of the liquid effluent. The TOC analysis confirmed this result. Typical results are illustrated in Table 4, which presents data for the gasification of sewage sludge.

CONCLUSION

Glucose as high as 22% by weight in water can be completely gasified to a hydrogen-rich gas with catalyst X at a WHSV as high as 22.2 (g/h)/g in supercritical water at 600°C, 34.5 MPa. Complete conversions of low concentrations of whole biomass feeds, including water hyacinth, depithed bagasse liquid extract, and sewage sludge, have also been achieved.

REFERENCES

- Baker, E. G., L. J. Sealock, Jr., R. S. Butner, D. C. Elliot, and G. G. Newenschwander (1989), "Catalytic destruction of hazardous organics in aqueous wastes: Continuous reactor system experiments," *Hazardous Waste & Hazardous Mat.*, **6**, 87-94.
- Dehui, Y., M. Aihara, and M. J. Antal, Jr. (1993), "Hydrogen production by steam reforming glucose in supercritical water," *Energy and Fuels*, **7**(5), 574-577.
- Elliott, D. C., E. G. Baker, R. S. Butner, and L. J. Sealock, Jr. (1993a), "Bench-scale reactor tests of low temperature, catalytic gasification of wet industrial wastes," *J. Sol. Energy Eng.*, **115**, 52-56.
- Elliott, D. C., L. J. Sealock, Jr., and E. G. Baker (1993b), "Chemical processing in high-pressure aqueous environments. 2. Development of catalysts for gasification," *Ind. Eng. Chem. Res.*, **32**, 1542-1548.
- Sealock, L. J. Jr., D. C. Elliott, E. G. Baker, and R. S. Butner (1993), "Chemical processing in high-pressure aqueous environments. 1. Historical perspective and continuing developments," *Ind. Eng. Chem. Res.*, **32**, 1535-1541.

Table 1. Temperature effect on the gasification of glucose in supercritical water with catalyst X (1.0 M glucose reactant, WHSV = 13.5 (g/h)/g, 34.5 MPa)

Temperature	600°C	550°C	500°C
Gas yields			
H ₂	1.97	0.62	0.46
CO	2.57	1.67	1.57
CO ₂	1.54	0.73	0.85
CH ₄	0.90	0.37	0.25
C ₂ H ₄	0.01	0.01	0.02
C ₂ H ₆	0.25	0.10	0.07
C ₃ H ₆	0.01	0.03	0.04
C ₃ H ₈	0.11	0.05	0.04
Carbon gasification efficiency	0.98	0.54	0.51
Tar yield	0.1%	0.9%	1.3%

Table 2. Glucose reactant concentration effect on the gasification efficiency in supercritical water at 600°C, 34.5 MPa, with catalyst X. (Flow rate: 1.0 cm³/min)

	1.2 M glucose with 0.6 g catalyst (WHSV = 22.2 (g/h)/g)	0.8 M glucose with no catalyst (Res. time = 28 s)
Gas yield		
H ₂	2.24	0.70
CO	0.79	1.63
CO ₂	3.09	2.01
CH ₄	1.23	0.75
C ₂ H ₄	0.00	0.04
C ₂ H ₆	0.35	0.22
C ₃ H ₆	0.00	0.04
C ₃ H ₈	0.13	0.09
Carbon gasification efficiency	1.03	0.88
Tar yield	0.008%	Not available

Table 3. Stability of catalyst X in a continuous run of glucose gasification in supercritical water at 600°C, 34.5 MPa (1.2 M glucose, WHSV = 19.9 (g/h)/g, catalyst X 2.55 g)

Time on stream	0.7 h	1.77 h	3.92 h	5.2 h
Gas yield				
H ₂	3.83	3.85	1.97	1.53
CO	0.79	0.63	2.41	2.71
CO ₂	3.32	3.49	1.84	1.18
CH ₄	0.95	0.94	0.93	0.83
C ₂ H ₄	0.00	0.00	0.01	0.01
C ₂ H ₆	0.26	0.26	0.25	0.21
C ₃ H ₆	0.00	0.01	0.01	0.02
C ₃ H ₈	0.15	0.13	0.11	0.09
Carbon gasification efficiency	1.00	1.00	1.01	0.91
Tar yield	0.02%	0.03%	0.07%	0.16%
TOC yield	1.4%	2.5%	5.4%	5.8%

Table 4. Sewage sludge gasification in supercritical water at 600°C, 34.5 MPa, with catalyst X (28 g/dm³ sewage sludge with 2.96 g catalyst X, WHSV = 0.50 (g/h)/g)

Gas product	Yield ^a	Mole fraction ^b
H ₂	2.7%	33%
CO	3.5%	2.9%
CO ₂	66.2%	36%
CH ₄	16.3%	24%
C ₂ H ₄	0.05%	0.04%
C ₂ H ₆	7.7%	5.7%
C ₃ H ₆	0.3%	0.15%
C ₃ H ₈	1.7%	0.89%
total	98.4%	
Liquid yield ^c	0.99%	
TOC analysis	0.28 g-carbon / dm ³	
Mass balance ^d	99.4%	

a Gas yield = weight of gas / weight of reactant

b Mole fraction = mole of gas / total mole of gas in the effluent

c Liquid yield = weight of solid residue in liquid / gram of reactant

d Mass balance = total gas yield + liquid yield

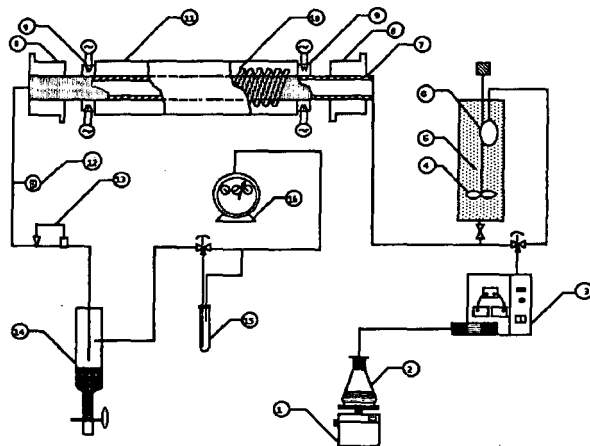


Fig. 1. Reactor system scheme. 1) Balance; 2) Flask with reactant; 3) HPLC pump; 4) Feeding vessel with agitator; 5) Wet-biomass slurry; 6) Balloon; 7) Inconel 625 tube; 8) Cooling jacket; 9) Heater; 10) Furnace; 11) Furnace shell; 12) Pressure transducer; 13) Back pressure regulator; 14) Gas sample output; 15) Liquid-gas separator; 16) Wet test meter

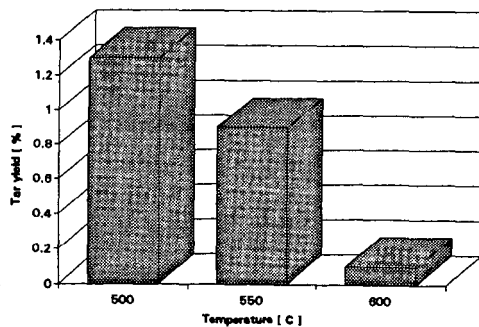


Fig. 2. Tar yield vs. reaction temperature (1.0M glucose reactant, WHSV = 13.5 (g/h)/g)